Science AAAS

Supplementary Materials for

Hyperexcitable arousal circuits drive sleep instability during aging

Shi-Bin Li *et al*.

Corresponding author: Luis de Lecea, llecea@stanford.edu

Science **375**, eabh3021 (2022)
DOI: 10.1126/science.abh3021

The PDF file includes:

Materials and Methods
Supplementary Text
Figs. S1 to S14

Other Supplementary Material for this manuscript includes the following:

MDAR Reproducibility Checklist

Materials and Methods

Animals

Experiments with mice were performed following the protocols approved by the Stanford University Animal Care and Use Committee in accordance with the *National Institutes of Health Guide for the Care and Use of Laboratory Animals*. Discomfort, distress, and pain were minimized with anesthesia and analgesic medications. Mice were housed in a temperature- and humidity-controlled animal facility with a 12-h/12-h light/dark cycle (9 am light on, Zeitgeber time 0/ZT 0), unless otherwise specified. Mice had ad libitum access to standard laboratory mouse food pellets and water. 2-3 month young male adult wild type (WT) mice were acquired from Jackson Laboratory (Jax) and 18 month old WT male mice were acquired from National Institute on Aging (NIA). OX(Hcrt)-ataxin3 heterozygotes (*15*), Hcrt-IRES-Cre knock-in (Hcrt::Cre) heterozygotes (*20*), OX(Hcrt)-eGFP heterozygotes (*29*) and tyrosine hydroxylase (TH)-IRES-Cre knock-in (TH::Cre) heterozygotes (European Mouse Mutant Archive; EMMA ID: EM:00254) (*49*) were backcrossed onto C57BL/6J background. Male mice were used in the experiments, unless otherwise specified. Mice at an age younger than 5 months belonged to the young group, whereas mice older than 18 months were considered as aged. Animals from multiple litters were randomly assigned to control or experimental group under each experimental paradigm. Group sizes were determined based on earlier publications (*13, 50, 51*).

EEG-EMG electrode preparation and implantation

Mini-screw (US Micro Screw) was soldered to one tip of an insulated mini-wire with two tips exposed, and the other tip of the mini-wire was soldered to a golden pin aligned in an electrode socket. A micro-ring was made on one side of an insulated mini-wire with the other end soldered to a separate golden pin in the electrode socket. Each electrode socket contained 4 channels with 2 mini-screw channels for EEG recording and 2 micro-ring channels for EMG recording as described in earlier work from our lab (*12, 47, 50*). The resistance of all the channels was controlled with a digital Multimeter (Fluke) to be lower than 1.5 ohms for ideal conductance. Mice were mounted onto an animal stereotaxic frame (David Kopf Instruments) under anesthesia with intraperitoneal injection of a mixture of ketamine (100 mg/kg) and xylazine (20 mg/kg). Two mini-screws were placed in the skull above the frontal (AP: -2 mm; ML: ± 1 mm) and temporal (AP: 3 mm, ML: ± 2.5 mm) cortices for EEG signal sampling and two micro-rings were placed in the neck muscles for EMG signal acquisition. Electrode socket was secured with Metabond (Parkell, Japan) and dental acrylic on skull for recording in freely moving mice. Buprenorphine SR (0.5 mg/kg) was administered subcutaneously to mice before and after surgery for pain relief. After surgery, revertidine (5 mg/kg) was administered (intraperitoneal) to mice to facilitate recovery from anesthesia.

Virus injection with and without fiber optic implantation

Optogenetic experiments: 0.3 μl AAV-DJ-EF1α-DIO-hChR2(H134R)-eYFP viruses (ChR2-eYFP, 6.5×10^{12} gc/ml, Stanford Virus Core, Lot no. 4176) was delivered to LH (AP: −1.35 mm, ML: ± 0.95 mm, DV: −5.15 mm) of anesthetized young (3 to 5 months) or aged (18 to 22 months) Hcrt::Cre mice with a 5 μl Hamilton microsyringe according to stereotaxic coordinates determined on a Kopf stereotaxic frame. AAV-DJ-EF1α-DIO-eYFP viruses (eYFP, 6.9×10^{12} gc/ml, Stanford Virus Core, Lot no. 3010) was used as control or for in vitro pharmacology experiments. A glass fiber (200 μm core diameter, Doric Lenses, Franquet, Québec, Canada) was implanted with the tip right above the injection site for optogenetic stimulations later on. After fixing the glass fiber with Metabond, the EEG/EMG electrodes were implanted with dental acrylic fixation. Similar procedure was performed for virus injection in TH::Cre mice targeting LC NA neurons (AP: – 5.46 mm, ML: ± 1.2 mm, DV: – 3.6 mm). Mice were allowed to recover for at least 2 weeks to get sufficient virus expression before connecting to the EEG/EMG recording cables and optical stimulation patch cord. EEG/EMG electrode and fiber optic implantation were omitted in the mice infected with ChR2-eYFP or eYFP viruses used for in vitro electrophysiology experiments.

Fiber photometry: For fiber photometry, 0.3 μl AAV vectors encoding GCaMP6f (AAV-DJ-EF1α-DIO-GCaMP6f, 1.1×10^{12} gc/ml, Stanford Virus Core, Lot no. 3725) were delivered to LH (AP: − 1.35 mm, ML: ± 0.95 mm, DV: − 5.15 mm) of young (3 to 5 months) or aged (18 to 22 months) Hcrt::Cre mice with a 5 μl Hamilton micro-syringe. A glass fiber (400 μm core diameter, Doric Lenses) was implanted with the tip at the injection site for GCaMP6f signal acquisition afterwards. EEG/EMG electrodes were implanted following fixation of fiber optic and secured with Metabond and dental acrylic. Mice were allowed to recover for at least 2 weeks to get sufficient virus expression before connecting to the EEG/EMG recording cables and fiber photometry recording patch cord.

Single-nucleus RNA-sequencing (snRNA-seq): To label telomeres in the nuclei, 0.3 µl AAV vectors encoding Cre-dependent DsRed-hTRF2 (*52*) (AAV-DJ-DIO-DsRed-hTRF2, 1.95×10^{12} gc/ml, customer viruses packaged at Stanford Virus Core, Lot no. 4422) were bilaterally injected to the LH (AP: −1.35 mm, ML: ± 0.95 mm, DV: −5.15 mm) of young (3 months) and aged (18 months) male and female Hcrt::Cre mice [3 mice per condition (young/aged male/female)].

EEG-EMG recording and analysis

Mice were singly-housed after surgery and allowed to recover for 1 week with access to food and water ad libitum before EEG/EMG recording. EEG/EMG signals were amplified through a multiple channel amplifier (Grass Instruments) and acquired with VitalRecorder (Kissei Comtec Co.) with a sampling frequency of 256 Hz followed by offline signal analysis. The bandpass was set between 0.1 and 120 Hz. Raw EEG/EMG data were exported to Matlab (MathWorks, Natick, MA, USA) and analyzed with custom scripts and Matlab built-in tools based on described criteria (*12*) to determine behavioral states. Cataplexy-like EEG/EMG pattern was determined based on the criteria described in the original publication reporting the OX(Hcrt)-ataxin3 narcolepsy mouse model (*15*) and the consensus definition of cataplexy in mouse models of narcolepsy: (i) ⩾ 10 sec of EMG atonia; (ii) EEG with theta band domination; (iii) behavioral immobility preceded by ⩾ 40 sec of wakefulness (*30*). For optogenetic and fiber photometry recording experiments, simultaneous EEG/EMG signals were recorded to determine behavioral states. The latency of sleep-to-wake transition and the duration of wakefulness following optogenetic stimulation during sleep were determined in SleepSign (Kissei Comtec Co.) with indication of stimulation timestamps on the raw EEG/EMG signals. EEG power spectral analysis was performed with the same method as described earlier (*13*). EEG band power calculation was based on: delta (1 to 4 Hz); theta (4 to12 Hz). EEG band power comparison between vehicle- and KCNQ2/3 ligand-treated groups was conducted based on signals during 1 hour (for vehicle versus XE991) and 3 hours (for vehicle versus flupirtine) following injection for wakefulness and NREM sleep based on the dynamic of drug's effect. As both XE991 and flupirtine postponed REM sleep onset, EEG band power was computed based on the initial REM sleep epoch after injection of vehicle/drug. The investigator was blind to the group information while conducting the EEG/EMG data analysis.

In vivo optogenetic stimulation

After recovery and sufficient virus expression (>2 weeks), mice injected with viruses expressing Cre-dependent ChR2-eYFP were connected to EEG/EMG recording cables and fiber optic patch cords (200 μm core diameter, Doric Lenses) for one week acclimation in special cages with open top which allowed mice to move freely. Following acclimation, optogenetic stimulation with a range of frequencies (1, 5, 10, 15, and 20 Hz, controlled by A.M.P.I. Master 8) and a range of blue light (473 nm) intensities (1, 5, 10, 15, and 20 mW, Laserglow Technologies, calibrated with Thorlabs light meter) was performed. Each stimulation train consisted of 15 ms light pulses for 10 sec with a given light intensity and frequency according to a randomized 5 (light intensities) × 5 (frequencies) matrix generated in Matlab. Sleep-to-wake transition experiments were performed between ZT5-ZT9 of their inactive phase when mice have a strong sleep pressure. Light stimulations were delivered to mice within 30 sec of NREM or REM sleep onset to determine the latency of sleep-to-wake transition and duration of wake bout following optogenetic stimulation. The onset of light stimulation was time-stamped during recording for offline analysis afterwards.

Fiber photometry signal acquisition and analysis

After recovery, sufficient virus expression (>2 weeks), and habituation to EEG/EMG cable and fiber optic patch cord (400 μm core diameter, Doric Lenses), mice injected with AAV viruses expressing Cre-dependent GCaMP6f were connected to EEG/EMG recording setup and a custom-built fiber photometry setup (*50*). Briefly, a 470 nm LED (M470D3, Thorlabs, NJ, USA) was sinusoidally modulated at 211 Hz and passed through a GFP excitation filter followed by a dichroic mirror (MD 498, ThorLabs) for reflection. The light stream was sent through a high NA (0.48), large core (400 μm) optical fiber patch cord (Doric Lenses, Québec, Canada), which was connected with a zirconia connector (Doric Lenses, Québec, Canada) to the dental acrylic-secured fiber optic implant (0.48NA, 400 μm, Doric Lenses, Québec, Canada) with the tip on the injection site. Separately, a 405 nm LED was modulated at 531 Hz and filtered by a 405 nm bandpass filter and sent through the optical fiber patch cord to mouse brain to evoke reference fluorescence, which was independent of Ca^{2+} release. GCaMP6f fluorescence and reference fluorescence were sampled by the same fiber patch cord through a GFP emission filter (MF525-39, ThorLabs), and center-aligned to a photodetector (Model 2151, Newport, Irvine, CA, USA) with a lens (LA1540-A, ThorLabs). The analog signals were amplified by two lock-in amplifiers for GFP fluorescence and reference fluorescence respectively (30 ms time constant, model SR380, Stanford Research Systems, Sunnyvale, CA, USA). Matlab-based custom software was used to control the LEDs and sample both the GFP fluorescence and reference fluorescence through a multifunction data acquisition device (National Instruments, Austin, TX, USA) with 256 Hz sampling frequency in a real-time manner. ΔF/F was obtained by subtracting the reference fluorescence signal from the 470 nm excited GFP emission signal to remove the system interference. The optical fiber patch cord was photobleached to minimize autofluorescence prior to recording according to the user manual (Doric Lenses, Québec, Canada). The recording was conducted between ZT5-ZT9 of their inactive phase when mice have a strong sleep pressure.

To reveal the Hcrt neuronal activity in driving behavioral pattern changes, we used a bottom-up analysis strategy, i.e., GCaMP6f data were staged independent of simultaneous EEG/EMG signals. We then separated the increased GCaMP6f into two categories: GCaMP6f transients during sleep (G^S) and GCaMP6f epochs associated with wakefulness (G^W) (Fig. 1). All the G^S and G^W were staged from the same amount of recording conducted during ZT5-ZT9 from equal group size (1 hour/each mouse, n = 6 mice each group) for comparison of Hcrt neuronal activity between young and aged mice. All the GCaMP ΔF/F transients with a Z score >1% (equals GCaMP6f ΔF/F value ~0.3-0.6 for individual animal) of the highest ΔF/F value of the entire trace were staged. After data staging, each GCaMP6f epoch was normalized to its own 5 sec baseline with time 0 defined for the beginning of GCaMP6f rising phase. Heatmaps were generated for each category based on 10 sec of normalized GCaMP6f epochs with 5 sec prior to and 5 sec after time 0. A Z score was calculated by subtracting the mean value of GCaMP6f trace prior to time 0 from the mean value of GCaMP6f after time 0 and an averaged Z score based on each animal was used for statistical comparisons. As the G^S Z score was generally small, only the G^S transients with Z score > mean (G^S Z score) – 3×SEM (G^S Z score) were included with ideal signal-to-noise ratio for subsequent analyses. By definition, all the G^W epochs were qualified for analyses. G^S scatter plot was generated with the duration of G^S against its peak value, and G^W scatter plot was generated with the duration of wake-associated G^W epoch against its maximum peak value (maximum GCaMP6f ΔF/F, if given epoch appeared with multipeaks). Animal-based frequencies of G^S and G^W were compared between the young and aged groups. Durations of sleep, wake, and S-W epochs were compared. Spearman correlation analysis with a linear fit was perform between G^W frequency (counts/hour) and mean sleep bout duration. The investigator was blind to the group information while conducting the GCaMP6f data staging.

Chemical preparation and application

XE991 dihydrochloride (Cat. no. 2000, referred to as XE991) and flupirtine maleate (Cat. no. 2867, referred to as flupirtine) were purchased from Tocris. XE991 was prepared in saline with a concentration of 50 µM for in vitro electrophysiology and prepared in saline with a concentration of 0.2 mg/ml for in vivo experiment with a dosage of 2 mg/kg (0.1 ml/10g, intraperitoneally). 5 mM flupirtine stock solution (0.9% saline containing 0.3% dimethyl sulfoxide/DMSO, v/v) was added to artificial cerebrospinal fluid (ACSF) to reach a concentration of 50 µM for in vitro electrophysiology. Flupirtine was prepared at a concentration of 2 mg/ml in 0.9% saline containing 0.3% DMSO (v/v, vehicle) for in vivo experiments with a dosage of 20 mg/kg (0.1 ml/10g, intraperitoneally). Flupirtine solution was ultrasonicated prior to application. Counterbalanced crossover design was used for in vivo pharmacology experiments to reveal the drug’s effect. Two rounds of drug administrations were separated by at least one week for a complete wash-out of drug’s effect. 4-Aminopyridine (4-AP) was purchased from Sigma-Aldrich (Cat. no. 275875). 100 mM 4-AP stock solution (0.9% sodium chloride/saline as vehicle) was added to ACSF to reach a concentration of 50 µM for in vitro electrophysiology of I_M experiment. MK6096 (Merck) was prepared at a concentration of 2 mg/ml in a mixture (v/v, vehicle) of 50% 0.9% saline and 50% Poly ethylene glycol (average Mn 400, PEG400, Sigma-Aldrich Cat. no. 202398) for in vivo pharmacology experiment as previously described (*13*).

In vitro electrophysiology

All the in vitro electrophysiology experiments were performed during the light phase (ZT3-ZT9). 3-9 mice were used each group. Slices were randomly assigned to groups examining effects of XE991 or flupirtine on M current in the in vitro pharmacology experiments.

Slice preparation: Mice from both groups were decapitated after anesthesia with sevoflurane or perfused with ice-cold slicing solution under anesthesia. To increase the chances of acquiring a healthy slice, we used a sucrose-based or choline-based ACSF for brain slice preparation to reduce the cell excitotoxicity and loss during slice preparation (*53*). After decapitation, the brain was rapidly dissected and immersed in ice-cold sucrose/choline-based ACSF slicing solution (pH 7.4, 95% O_2 / 5% CO_2). 300 µm-thick coronal brain slices containing Hcrt neurons with eYFP fluorescence were sectioned using a VT1200s vibratome (Leica Microsystems). After ~20 min incubation at ~35 ºC, the slices were stored at room temperature. Slices were used for maximally 5 hours after dissection. Experiments were performed at room temperature 21º to 24 ºC.

Recording and data analysis: During experiments, slices were superfused with a physiological extracellular solution containing: 125 mM NaCl, 2.5 mM KCl, 25 mM $NaHCO_3$, 1.25 mM NaH_2PO_4, 25 mM D-glucose, 2 mM $CaCl_2$, and 1 mM $MgCl_2$ (pH 7.4 in 95% O_2 / 5% CO_2, ~325 mOsm). Neurons were chosen based on eYFP expression and visualized with an Olympus BX51WI with Nomarski optics connected to a camera (Q-imaging). Thick wall borosilicate pipettes (1B150F-4, World Precision Instruments Inc.) were pulled using a P-97 puller (Sutter Instruments) and electrodes with a resistance of 3-6 megohms were used for recording. Intracellular solution used for whole-cell recording contained: 120 mM K-methyl-sulfonate, 10 mM NaCl, 10 mM EGTA, 1 mM $CaCl_2$, 10 mM HEPES, 0.5 mM NaGTP, 5 mM MgATP, pH adjusted to 7.2 with KOH, osmolarity adjusted to 305 mOsm with sucrose; 0.2% biocytin was added for post-hoc staining. Neurons were recorded under current-clamp to examine excitability, or under voltage-clamp to examine PSCs. 1 sec step currents from -50 pA to 300 pA were used to evoke AP firing. For optogenetic stimuli, a 15 ms blue light pulse (3.4 mW, calibrated with Thorlab light meter) was given at 1 Hz, 5 Hz, 10 Hz, 15 Hz and 20 Hz in a randomized manner for 10 sec to compare light-induced activity between the young and aged groups, and the interval between sweeps was 20 sec. Data were acquired with a Multiclamp 700B amplifier (Axon Instruments, USA), and sampled at 10 kHz. Stimulus generation and data acquisition were performed using pClamp 10. Data were analyzed using Stimfit 0.14.9 (www.stimfit.org) and R 3.5.1 (the R project for statistical computing). RMP values were measured and averaged from temporal windows (at least 50 ms prior to the peak of a given AP for spontaneously firing neurons) with minimal membrane potential variance (*54*). The RMPs were determined without predicted/measured junction potential correction. All the amplitudes of APs and spikelets were calculated from RMPs. Depolarization events with a peak value above – 20 mV, and with a half width shorter than 6 ms were qualified for spikelet analyses. PSC recording from non-fluorescent neuron innervated by fluorescent Hcrt neuron expressing ChR2-eYFP was performed as illustrated in fig. S4A. For the PSC failure analysis, a success PSC was considered when a current deflection bigger than 10 pA occurred time-locked to the light pulse. The investigators were blind to the group information while conducting the data analyses.

LC neurons were recorded in slices prepared from WT young (2 to 3 months) and aged (18 to 21 months) mice, infused with biocytin, followed by antibody staining against tyrosine hydroxylase (TH). Only the neurons positive for both biocytin and TH were included for data analyses.

I_M recording: For recording of the slowly deactivating M-current (I_M) mediated by KCNQ2/3, perforated patch recordings were used to maintain the integrity of second messenger signaling cascades and minimize current rundown. The pore-forming antibiotic nystatin was dissolved in DMSO at 50 mg/ml. This stock solution was diluted in an internal pipette solution and vortexed and ultrasonicated for a final concentration of 100 to 200 µg/ml. Pipette tips were prefilled by brief immersion into antibiotic-free solution and then pipettes were back filled with nystatin. After the cell-attached configuration was attained, the access resistance was periodically monitored with hyperpolarizing voltage steps (10 mV, 20 ms) and capacitative transients were cancelled. After 10 to 20 minutes, recording was started once the access resistance stabilized. The

recording was terminated if a sudden change in access resistance occurred. Extracellular solution contained 4-AP (5 mM) to minimize contamination by other potassium currents, and AMPARs, glycine receptors and $GABA_A$ receptors were blocked by 6,7-dinitroquinoxaline-2,3-dione (DNQX, Tocris Cat. no. 0189, 10 μM), strychnine (Sigma-Aldrich Cat. no. S0532, 1 μM), (2R)-amino-5-phosphonopentanoate (APV, Tocris Cat. no. 0106, 100 μM) and bicuculline (Sigma-Aldrich Cat. no. 285269, 10 μM). I_M was recorded using a standard deactivation protocol (1000 ms hyperpolarizing steps to -30 mV from a holding potential of -20 mV every 10 sec, inter-sweep holding potential – 20 mV). I_M did not inactivate with this protocol, while contamination by other voltage-gated currents was minimized. I_M was measured as the inward relaxation current caused by deactivation of I_M during this voltage step (Fig. 4, G and H). After obtaining at least a stable 5 min baseline, XE991 (50 μM) or flupirtine (50 μM) was applied. The effect of XE991 or flupirtine was determined by comparing averaged I_M amplitudes over a 5 min period just before XE991 or flupirtine application with averaged I_M amplitudes during the 5 to 10 min period after XE991 or flupirtine application.

Array tomography (AT)

Tissue preparation: Array creation and immunohistochemistry were described in detail in a previous publication (*55*). In short, a small piece of tissue (~2 mm high by 1 mm wide by 1 mm deep), covering the LH containing eYFP-labeled Hcrt neurons, was microwave-fixed in 4% Paraformaldehyde (PFA). The fixed tissue was then dehydrated in graded steps of ethanol, and then embedded in LR White resin overnight at 50 °C. The embedded tissue was sectioned on an ultramicrotome at a thickness of 70 nm and placed as a ribbon array directly on gelatin or carbon coated glass coverslips. The ultrathin physical sectioning allows AT to achieve true isotropic voxels of ~100 nm. To assure that the brain tissue from animals were prepared and imaged in as similar conditions as possible, all samples were paired starting at the tissue preparation step. Thus, young and aged animals were prepared in tandem, placed on the same coverslip, stained together and imaged together. Furthermore, to minimize the impact of locational differences in the gathered tissue, multiple blocks were generated from LH of each mouse, and screened at 20× using 4′,6-diamidino-2-phenylindole (DAPI) fluorescence. Then similar tissue blocks were used for further analysis.

Immunohistochemistry: Immunohistochemistry was then carried out on the arrays using primary antibody against KCNQ2 (Alomone Cat. no. AGP-065). The primary antibodies were visualized via fluorescence-labeled secondary antibody: (Alexa 594, Invitrogen Cat. no. A11076), and mounted in SlowFade Gold antifade with DAPI (Invitrogen Cat. no. S36938).

Microscopy: Wide-field imaging of ribbons were accomplished on a *Zeiss* Axio Imager.Z1 Upright Fluorescence Microscope with motorized stage and Axiocam HR Digital Camera as previously described (*56*). A position list was generated for each ribbon array of ultrathin sections using custom software modules written for Axiovision. Single fields of view were imaged for each position in the position list using a *Zeiss* 63×/1.4 NA Plan-Apochromat objective.

Image Registration and Processing: Image stacks from AT were imported into Fiji (ImageJ) and aligned using both rigid and affine transformations with the Register Virtual Stacks plugin. The aligned image stacks were further registered across image sessions using Fiji and TrackEM. The aligned and registered image stacks were imported into Matlab and deconvolved using the native implementation of Richardson-Lucy deconvolution with empirical or theoretical PSFs with 10 iterations (*56*). Custom functions were written to automate and facilitate this workflow.

eYFP Segmentation: eYFP delimited protein amount was calculated using custom Matlab software. eYFP volumes were slightly dilated via morphological operations and used to segment protein data in image space. Segmentation custom functions were used to quantify the number and amount of proteins encapsulated by eYFP.

Single-nucleus isolation, FACS sorting, RNA library preparation and sequencing

3 weeks after virus injection, mice were deeply anesthetized using isoflurane and perfused with 1× PBS. The brains were rapidly dissected and transferred to a chilled metal Brain Slicer Matrix (Zivic Instruments, 500 μm coronal slice intervals), and the brain sections containing Hcrt neurons (AP: – 1.0 ~ – 2.0 mm) were sliced and transferred to 1× PBS on ice. Bilateral hypothalamic areas (LH) were identified and dissected under a stereoscope. LH tissue blocks were then transferred to a glass dounce homogenizer (Sigma-Aldrich) on ice

and homogenized in 1 ml Homogenization Buffer (*57*) containing Tris (pH 8.0, 10 mM), sucrose (250 mM), KCl (25 mM), $MgCl_2$ (5 mM), Triton-X100 (0.1%), RNasin Plus RNase Inhibitor (0.5%, Promega Cat. no. N2615), SUPERase·In™ RNase Inhibitor (0.5%, ThermoFisher Cat. no. AM2694), Protease Inhibitor Cocktail (1×, Promega Cat. no. G6521), DTT (0.1 mM) and DAPI (1:1000, Invitrogen Cat. no. D3571). LH tissue blocks from 3 mice per condition (young/aged male/female) were pooled each condition for isolation of nuclei. The nuclei were released by sequentially applying 10 to 12 strokes of the loose dounce pestle and 10 to 12 strokes of the tight dounce pestle on ice, followed by filtering the suspension through a 35 μm cell strainer (Falcon). The nuclei were then spun down by centrifugation (10 min, 900× g at 4 ℃) and resuspended in the Wash Buffer (1× PBS containing 0.8% BSA, 0.5% RNasin Plus RNase Inhibitor and 0.5% SUPERase·In™ RNase Inhibitor). The single-nucleus suspension was further washed twice in Wash Buffer by centrifugation (10 min, 900× g at 4 °C). Fluorescence activated cell sorting (FACS) was performed using the 70 μm nozzle and optimal gates collecting the DsRed/DAPI double positive events and excluding debris and doublets. Sorted DsRed+ single nuclei were confirmed using a fluorescence microscope, and manually counted using a hemocytometer. snRNA-seq libraries were prepared using 10x Genomics Chromium Single Cell 3' Reagents v3 following manufacturer's instructions. Briefly, the concentration of single nuclei solution prepared from dissected LH tissue was determined using DAPI staining and Trypan Blue staining. The nuclei solution was loaded onto a Chromium Chip B to capture seven to ten thousand nuclei in droplets containing the reverse transcription reagents. After reverse transcription, the now barcoded cDNA was recovered and amplified for 12 polymerase chain reaction (PCR) cycles. After qualitative and quantitative control of the cDNA, the final libraries were constructed by fragmenting the cDNA, End Repair, and A-Tailing. After adapter ligation, the libraries were amplified for 11 PCR cycles. The libraries were sequenced using an Illumina MiSeq v3 150-cycle kit to check library quality and confirm the number of captured nuclei. Then all the barcoded samples were mixed and deep sequenced on an Illumina HiSeqX sequencing machine across 4 different lanes to avoid lane variability and potential lane failure.

snRNA-seq data analysis

Illumina fastq files were processed through the 10x Genomics cellranger pipeline according to the manufacturer's instructions. Briefly, reads were aligned to the mm10 mouse genome using a custom gtf annotation file which labeled all 'transcripts' as 'exons', thus allowing to count intronic as well as exonic reads. The four libraries were then combined using cellranger *aggr* command to match sequencing depth per cell across libraries. All further processing of the genes X cells count matrix was performed in Seurat V3 (*58*) using scTransform normalization (*59*). First, the population of Hcrt+ neurons were identified out of all sequenced cells by coarse Louvian clustering of the entire sequencing dataset. Only one cluster showed Hcrt expression. This cluster was then separately subclustered, and all doublet clusters were removed. No large batch effects were observed at this level. A core set of three clusters, all of which expressed Hcrt at high levels, served as the basis for the analysis of age related effects.

CRISPR/SaCas9-mediated Kcnq2/3 gene disruption in Hcrt neurons

The target sites of *Kcnq2/3* genes for Staphylococcus aureus CRISPR/Cas9 (CRISPR/SaCas9) were designed by CHOPCHOP (http://chopchop.cbu.uib.no) (*60*). The target sequences were as follows: sgKcnq2: 5′-CGCGTGTGGAGTCGGGCGCGC-3′, sgKcnq3: 5′-GCGGCCACCGCCCTCCAGCAG-3′. Oligonucleotides encoding guide sequences were purchased from Sigma-Aldrich and cloned individually into BsaI fragment of pX601 (Addgene plasmid 61591). U6-sgKcnq2 and U6-sgKcnq3 fragments were PCR-amplified, respectively using pX601-sgKcnq as a template. Amplified fragments were cloned tandemly into MluI-digested pAAV CAG FLEX mCherry by Gibson assembly method. The primers used were as follows; Gibson1-F: 5′-TAGGGGTTCCTGCGGCCGCAGAGGGCCTATTTCCCATG-3′, Gibson1-R: 5′-ATAGGCCCTCTCTAGAAAAAATCTCGCCAAC-3′, Gibson2-F: 5′-TTTTTCTAGAGAGGGCCTATTTCCCATG-3′, Gibson2-R: 5′-TCATTATTGACGTCAATGGAAAAAATCTCGCCAACAAGTTG-3′. AAV constructs carrying non-targeting guide sequences (5′-GCGAGGTATTCGGCTCCGCGT-3′) were used as control. For the Cre-dependent SaCas9 construct, SaCas9 fused with 3× HA tag was PCR amplified using pX601 as a template. Amplified fragment was cloned into AscI/NheI-double digested pAAV-U6-SaCas9gRNA(SapI)-CMV-

SaCas9-DIO-pA (Addgene plasmid 113691). Next, the plasmid was digested by MluI and applied to self-ligation to remove U6 promoter and single-guide RNA (sgRNA) scaffold sequences. pAAV CMV-DIO-SaCas9-3HA (SaCas9), pAAV U6 sgKcnq2-U6 sgKcnq3 CAG FLEX mCherry (sgKcnq2/3) and pAAV U6 sgControl-U6 sgControl CAG FLEX mCherry (sgControl) were packaged into AAV-DJ by the Wu Tsai Neurosciences Institute Gene Vector and Virus Core at Stanford University.

20 young (6 to 8 weeks old) Hcrt::Cre mice were separated into two groups in a random manner (n = 10/group). Under anesthetics and analgesic, according to the Hcrt neuron field coordinates as described above, one group received bilateral stereotaxic injection of a 0.6 µl (each side, 0.3 mm apart in depth) mixture of SaCas9 (2.4×10^{13} gc/ml) and sgControl (6.24×10^{12} gc/ml) and implanted with EEG/EMG electrodes to serve as the control group. The other group received bilateral stereotaxic injection of a 0.6 µl mixture of SaCas9 and sgKcnq2/3 (2.97×10^{12} gc/ml) and implanted with EEG/EMG electrodes to monitor the effect of Hcrt neuron-selective *Kcnq2/3* gene disruption on sleep architecture. After surgery, mice were connected to EEG/EMG recording cables and singly-housed with food and water ad libitum to recover, and for EEG/EMG signal recording. EEG/EMG signals were recorded continuously on day 6 and day 7 weekly up to 8 weeks (EEG/EMG recording lasted until 12 weeks in half of each group) after surgery. Following recording in week 8/12 after virus injection, slices were prepared from each group for in vitro electrophysiology experiment to determine RMP and firing property of the Hcrt neurons labeled by mCherry flag. Patch clamp recorded cells were infused with biocytin for subsequent immunostaining. The data were used for statistical analysis only if the recorded neurons were stained to co-express biocytin and HA tag.

Histology

For in vivo experiments, upon accomplishment of recordings, mice were perfused under anesthesia described above with ice-cold 1× PBS and followed by 4% PFA for immunostaining against Hcrt1/OXA for Hcrt neurons, and TH for LC NA neurons. Brains were rapidly extracted, postfixed with 4% PFA at 4 °C overnight, and equilibrated in 30% sucrose in 1× PBS containing 0.1% NaN_3. Then, brains were sectioned at – 22 °C with a cryostat (Leica Microsystems) at a thickness of 35 µm. Slices were collected from anterior to posterior consecutively to 24-well plates containing PBS with 0.1% NaN_3, covered with aluminum foil, and stored at 4 °C until immunostaining and imaging. Primary antibody against OXA/Hcrt1 (SC-8070, Lot no. A2915, Goat polyclonal IgG) was purchased from Santa Cruz Biotechnology. Primary antibody against TH (Chicken polyclonal anti-peptide, Cat. TYH, Lot no. TYH1897983) was purchased from Avēs. Primary antibody against HA tag (Rabbit Anti-HA tag pAb, Item no. 561, Lot no. 067) was purchased from MBL International Corporation. Secondary antibodies: Alexa Fluor 488 Goat anti-chicken IgG (H+L, Ref. no. A11039, Lot no. 1094413), Alexa Fluor 488 donkey anti-goat IgG (H+L, Ref. no. A11055, Lot no. 1869589), Alexa Fluor 488 donkey anti-rabbit IgG (H+L, Ref. no. A21206, Lot no. 1910751), Alexa Fluor 647 donkey anti-goat IgG (H+L, Ref. no. A21447, Lot no. 2175459), were purchased from Invitrogen (Manufacturer: Life Technologies). Alexa Fluor 594 streptavidin conjugate (Ref. no. S11227, Lot no. 1991448) and Alexa Fluor 647 streptavidin conjugate (Ref. no. S32357, Lot no. 1738557) to label neurons infused with biocytin were purchased from Invitrogen. For the WT mice used for comparison of sleep patterns, sections around LH and LC were washed in 1× PBS for 5 minutes, 3 times and incubated in a blocking solution of PBS with 0.3% Triton X-100 (PBST) and 4% bovine serum albumin (BSA) for 1 hour. Following that, OXA/Hcrt1 primary antibody was added to the blocking solution (1:800) overnight. On the second day, sections were washed in 1× PBS for 3 times (5 min/time), and incubated in blocking buffer for 2 hours. After blocking, secondary antibody was added to the blocking buffer for 2 hours (dilution 1:800). After 3 times of 5-min 1× PBS washing, brain sections were mounted onto gelatin-coated slides, covered with Fluoroshield containing DAPI mounting media (Sigma-Aldrich, F6057) and cover glass for imaging with wild field microscope (Zeiss AxioImager, Germany) for entire section or LSM710 Confocal Microscope for enlarged visualization (Zeiss, Germany). For brain slices infected with Cre-dependent viruses, slices around the injection site were collected and stained with appropriate antibodies as described above. Alexa Fluor 594 streptavidin conjugate or Alexa Fluor 647 streptavidin conjugate for staining of biocytin was added together with the secondary fluorescent antibody for Hcrt1, TH or HA tag on the second staining day for in vitro experiment slices.

Object recognition test

Aged mice (~20 months, singly-housed with a reversed 12-h/12-h light/dark cycle, 9 pm light on, Zeitgeber time 0/ZT 0) were used to evaluate flupirtine's effect on memory ability in the object recognition task. The object recognition task was performed according to a protocol described by Leger et al. (*61*). The protocol consisted of habituation, familiarization and test sessions (fig. S8). During each habituation session, an individual mouse was released to the arena (34 cm × 17 cm, non-transparent open field filled with Sani-Chip pine bedding floor) for habituation of 5 min. Each mouse underwent two habituation sessions conducted during ZT16-18 and ZT22-24 for 3 consecutive days. During the familiarization session (Day 4: ZT22-24), each mouse was allowed to explore two identical objects for a total of 5 min. Each object was placed at the same distance from the walls and corners of the field without spatial or odor cues (bedding was changed; arena and objects were cleaned with 70% ethanol before each exposure). After the familiarization session, mice were intraperitoneally injected with either vehicle or flupirtine (20 mg/kg) at the beginning of the following light phase. During the test session (Day 5: ZT22-24), mice were placed in the same arena with one of the familiar objects from the familiarization session replaced by a similar size novel object. The position of the novel object (left or right) was randomized for each mouse and each group tested. Time spent facing away from object within the 7 cm radius or climbing on object was not qualified as exploration. Mice were randomly assigned to control/flupirtine group through a counterbalanced crossover design. Two rounds of object recognition task (with two sets of familiar and novel objects) were separated by one week for a complete drug wash-out. Animal-based averaged value of two rounds of familiarization was presented. Mouse with over 65% preference for either object during the familiarization session was not qualified to proceed to the next session.

Statistics

One/two hour-binned sleep comparisons were analyzed by two-way repeated measure (RM) analysis of variance (ANOVA) (linear mixed-effects model for counterbalanced crossover design) followed by Šidák's multiple comparisons. Holm-Šidák was used for comparison based on 24 h/light/dark phase. Unpaired *t*-test with Welch's correction was used for GCaMP6f data and in vivo optogenetic data analyses. For slice electrophysiology, Mann-Whitney *U* test, RM one-way ANOVA, two-way ANOVA were used to analyze appropriate datasets. Paired test was used for data analyses of experiments with paired design. Spearman correlation with a linear fit was performed for 2-demensional data correlation analysis. For snRNA-seq data, differentially expressed genes across ages were determined using the Wilcoxon rank-sum test, considering only those genes with a Bonferroni adjusted $P < 0.05$. Differences with $P < 0.05$ were considered significant for all experiments. In figures, *, **, ***, ****, and † indicate $P < 0.05$, $P < 0.01$, $P < 0.005$, $P < 0.001$, and $P < 0.0005$, respectively, and ns indicates not significant. Data with error bars were reported as mean ± SEM. Details on statistical analyses have been described in the supplementary text.

figs. S1 to S14

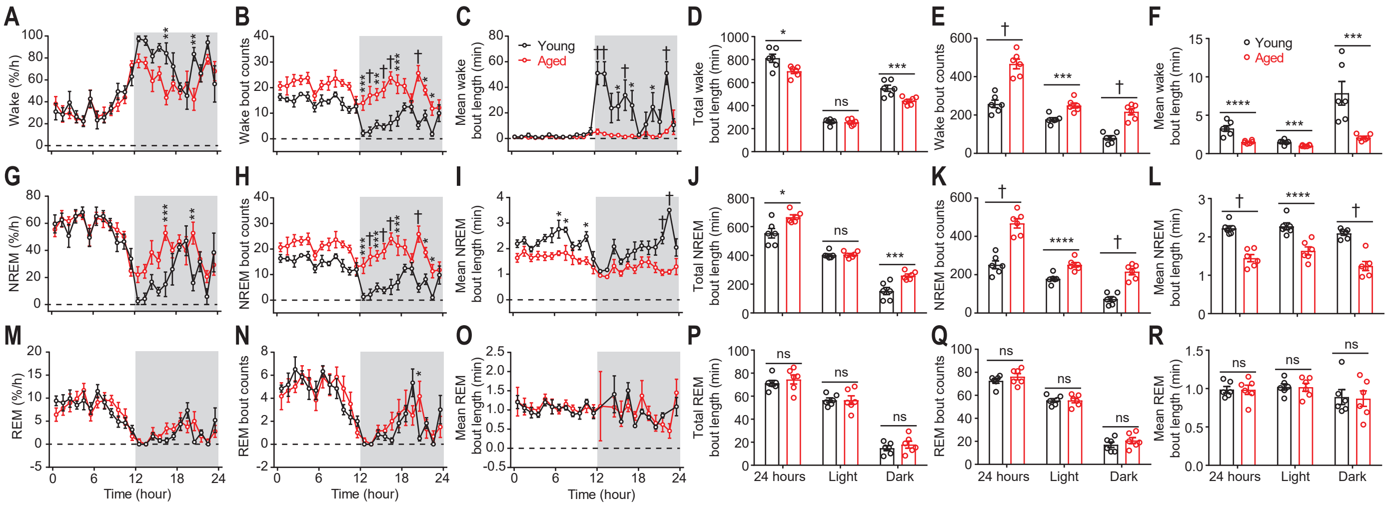

fig. S1. Comparison of sleep/wake patterns between young (3 months) and aged (20 months) mice. (**A** to **F**) Comparison of (A) hourly-based percentage, (B) hourly-based bout counts, (C) hourly-based mean bout length, (D) total bout length, (E) total bout counts, and (F) mean bout length of wakefulness between young and aged mice. (**G** to **L**) Comparison of (G) hourly-based percentage, (H) hourly-based bout counts, (I) hourly-based mean bout length, (J) total bout length, (K) total bout counts, and (L) mean bout length of NREM sleep between young and aged mice. (**M** to **R**) Comparison of (M) hourly-based percentage, (N) hourly-based bout counts, (O) hourly-based mean bout length, (P) total bout length, (Q) total bout counts, and (R) mean bout length of REM sleep between young and aged mice. Data indicate mean ± SEM (A to C, G to I, M to O: two-way RM ANOVA followed by Šidák's multiple comparisons, dark phase indicated by gray shielding; D to F, J to L, P to R: Holm-Šidák; *$P < 0.05$, **$P < 0.01$, ****$P < 0.005$, ****$P < 0.001$, †$P < 0.0005$; n = 6 mice each group; statistical details are available in the supplementary text).

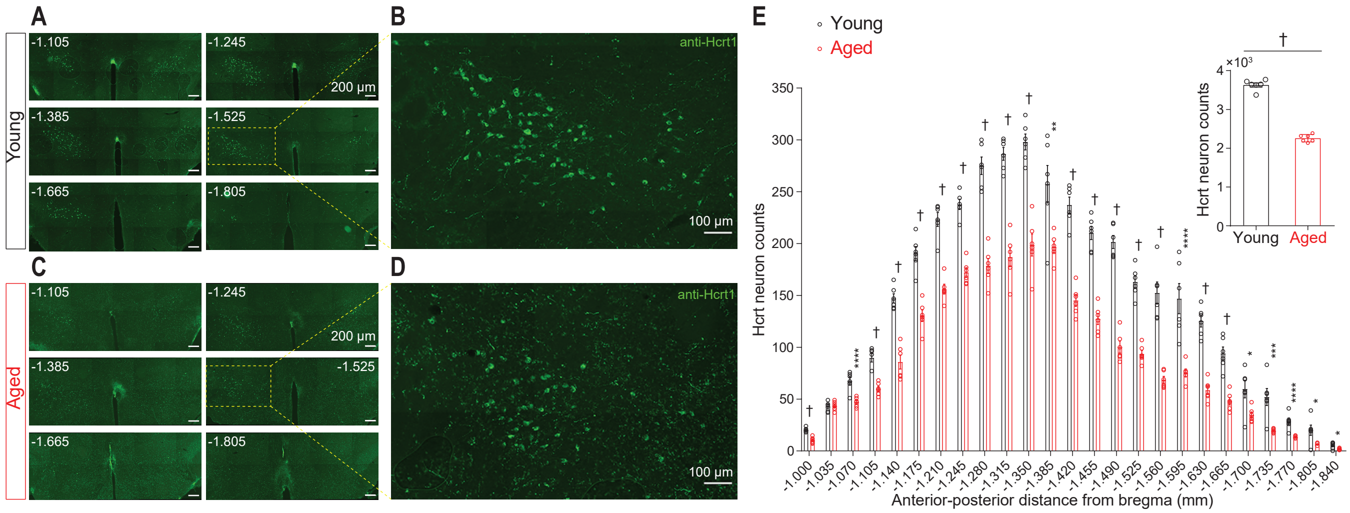

fig. S2. Significant Hcrt neuron loss in aged mice. (**A** and **B**) Antibody staining against Hcrt1 in brain slices spanning anterior-posterior (from bregma) –1.000 mm to –1.840 mm from a young mouse. (A) Representative young slices spaced by 0.140 mm, and (B) magnified display of the boxed region in panel A. (**C** and **D**) Antibody staining against Hcrt1 in brain slices spanning anterior-posterior (from bregma) –1.000 mm to –1.840 mm from an aged mouse. (C) Representative aged slices spaced by 0.140 mm, and (D) magnified display of the boxed region in panel C. (**E**) Anterior-posterior location-matched comparison of Hcrt neuron counts, and (inset) total Hcrt neuron counts between the young and aged groups. Data indicate mean ± SEM (n = 6 mice each group; two-way ANOVA followed by Šidák's multiple comparisons; inset: unpaired *t*-test; **P* < 0.05, ***P* < 0.01, ****P* < 0.005, *****P* < 0.001, †*P* < 0.0005; statistical details are available in the supplementary text).

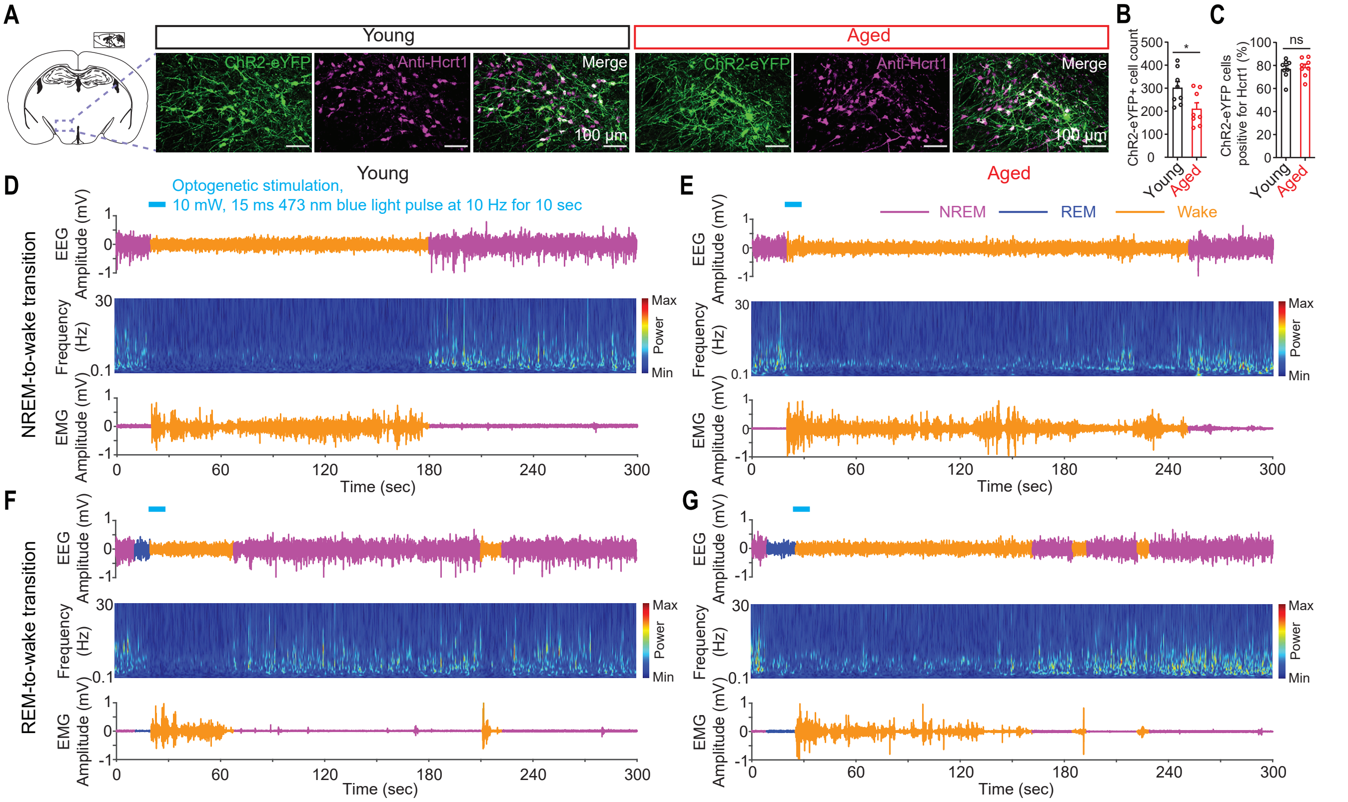

fig. S3. Representative EEG-EMG traces for sleep-to-wake transitions upon optogenetic stimulation of Hcrt neurons expressing ChR2-eYFP in young and aged Hcrt::Cre mice. (**A**) Representative LH slices containing neurons expressing ChR2-eYFP beneath the optical stimulation fiber tip stained with antibody against Hcrt1 from the young and aged groups. (**B** and **C**) (B) Less ChR2-eYFP-expressing neurons in the aged group and (C) comparable fractions of ChR2-eYFP expressing neurons positive for Hcrt1 staining in the young and aged groups (n = 8 mice each group, Mann-Whitney *U* test; statistical details are available in the supplementary text). (**D** and **E**) Representative traces for sleep-to-wake transitions upon optogenetic stimulation of Hcrt neurons during NREM sleep in (D) a young and (E) an aged Hcrt::Cre mouse respectively. (**F** and **G**) Representative traces for sleep-to-wake transitions upon optogenetic stimulation of Hcrt neurons during REM sleep in (F) a young and (G) an aged Hcrt::Cre mouse respectively.

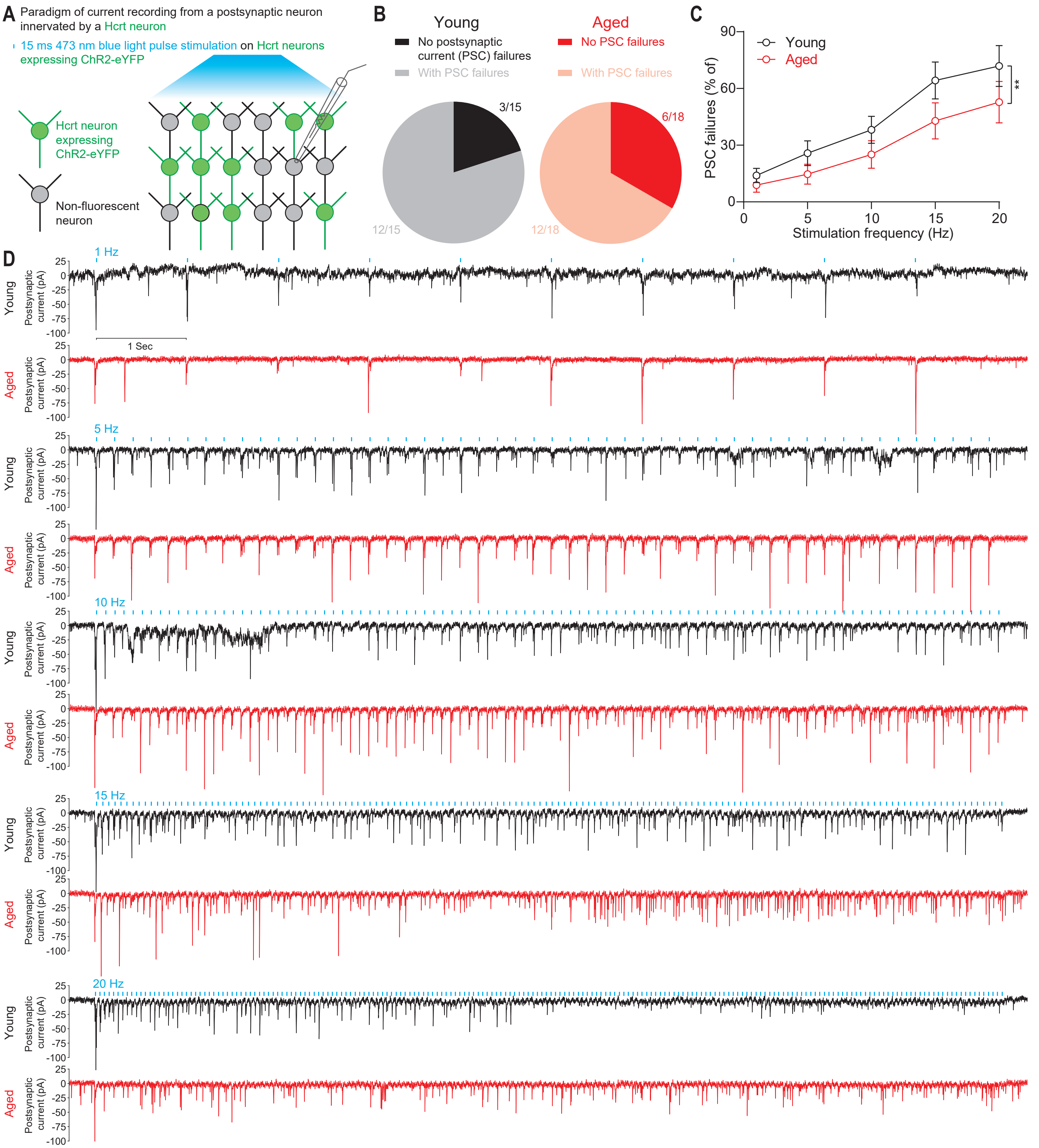

fig. S4. Voltage-clamp recording from non-fluorescent neurons during optogenetic stimulation of Hcrt neurons in the same slice. (**A**) Schematic of patch clamp recording from a non-fluorescent neuron innervated by a fluorescent ChR2-eYFP expressing Hcrt neuron in a brain slice. (**B** and **C**) (B) Fractions of young and aged Hcrt postsynaptic neurons with/without PSC failures following optogenetic stimulation of Hcrt neurons at (C) different frequencies (young: n = 15 neurons from three mice versus aged: n = 18 neurons from three mice). (**D**) Representative synaptic current traces recorded from young and aged neurons while optogenetically stimulating ChR2-eYFP-expressing Hcrt neurons in slices. Data indicate mean ± SEM [(C) two-way ANOVA followed by post-hoc Šidák's multiple comparisons; ***P* <0.01; statistical details are available in the supplementary text].

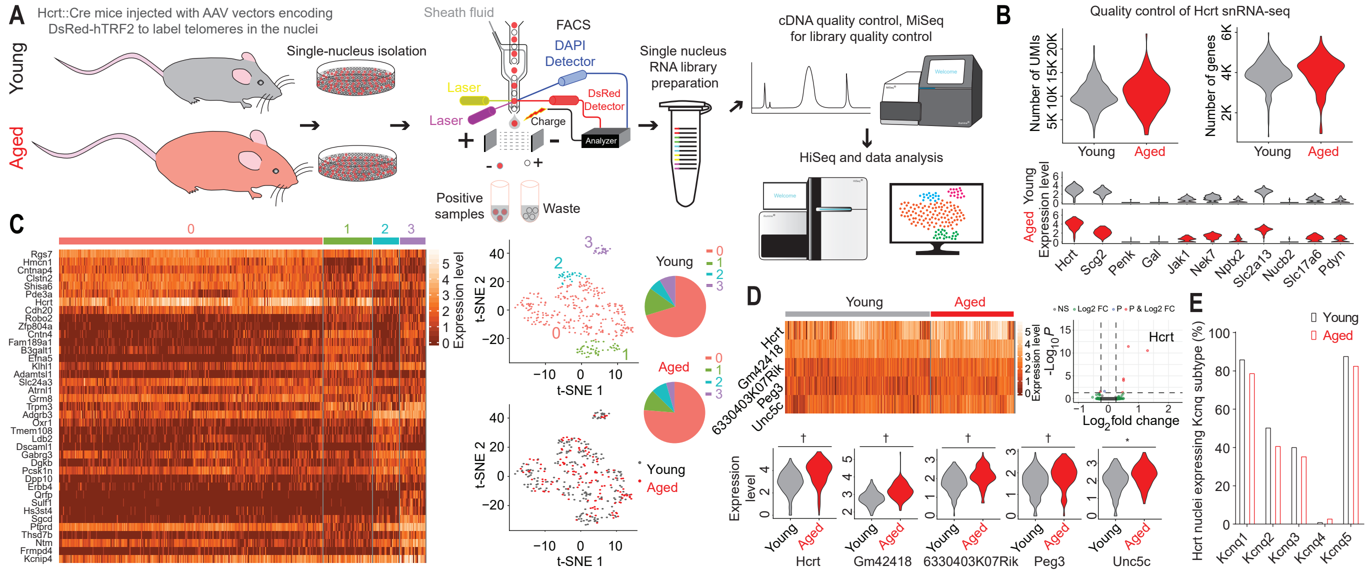

fig. S5. Single-nucleus RNA-sequencing of Hcrt neurons from young and aged male Hcrt::Cre mice. (**A**) Flowchart of single-nucleus RNA library preparation, quality control, sequencing and data analysis. (**B**) Sequencing data quality control. (top left) Comparable sequencing depth and (top right) numbers of genes between young and aged Hcrt nuclei. (bottom) Similar expression profiles of representative genes in young and aged Hcrt nuclei. (**C**) (left) Gene expression level for t-SNE plot showing (middle top) 4 distinct Hcrt neuron clusters, and (middle bottom) young and aged Hcrt nuclei distribute similarly among these clusters. (right) Comparable fractions of each cluster in young and aged Hcrt nuclei. (**D**) Genes expressed with significant differences between young and aged Hcrt nuclei. (top left) Heatmap of individual Hcrt nucleus with gene expression level; (top right) volcano plot of regulation significance $-\text{Log}_{10}P$ against expression Log_2 fold change (FC) with expression level normalized to young Hcrt dataset; (bottom) significantly upregulated genes in aged Hcrt nuclei (Wilcoxon rank-sum test, considering only those genes with a Bonferroni adjusted $P < 0.05$; $*P < 0.05$, $†P < 0.0005$; statistical details are available in the supplementary text). (**E**) Percentage of Hcrt nuclei expressing *Kcnq* subtypes in young and aged male mice. Note the lower percentage of aged Hcrt nuclei actively expressing the dominant subtypes *Kcnq1/2/3/5*.

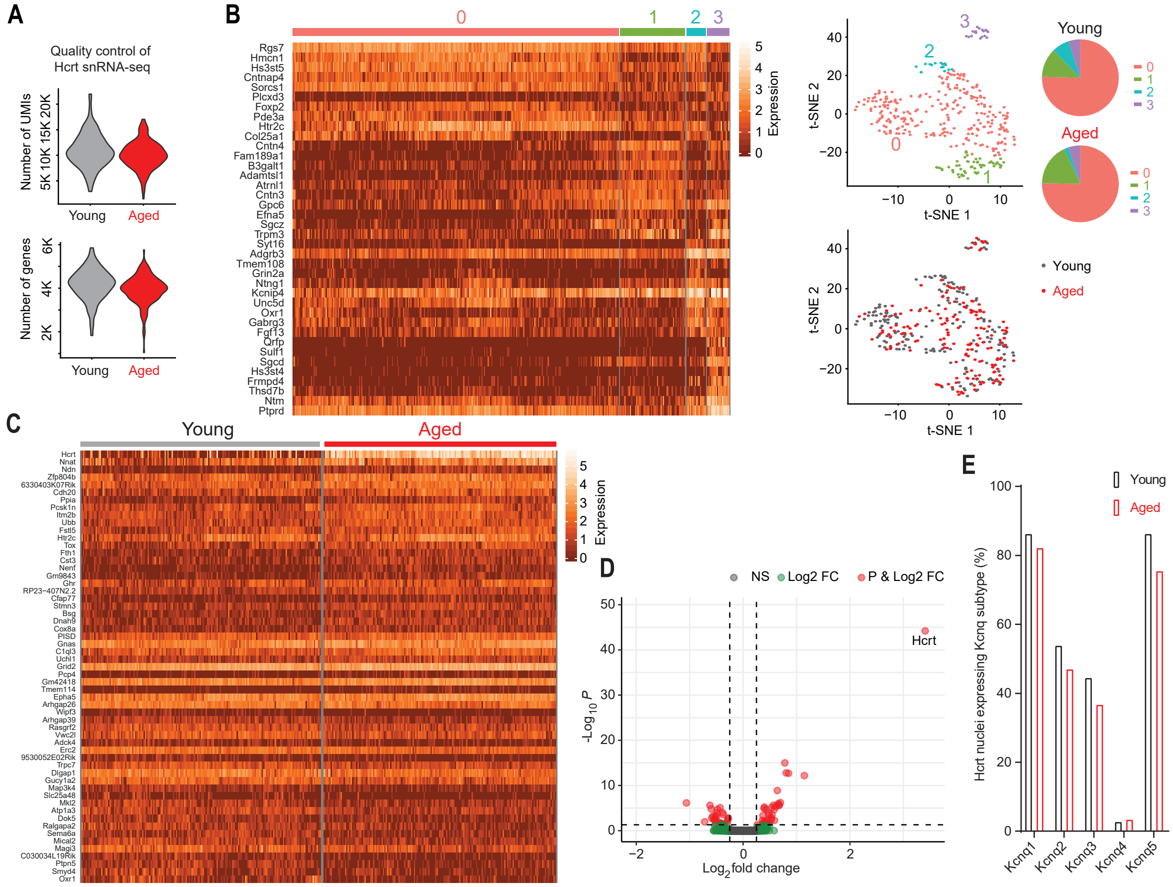

fig. S6. snRNA-seq of Hcrt neurons from young and aged female mice. (**A**) Sequencing data quality control. Comparable sequencing depth, numbers of genes between young and aged Hcrt nuclei. (**B**) (left) Gene expression level for t-SNE plot showing (middle top) 4 distinct Hcrt neuron clusters, and (middle bottom) young and aged Hcrt nuclei distribute similarly among these clusters. (right) Comparable fractions of each cluster in young and aged Hcrt nuclei. (**C**) Genes expressed with significant differences between young and aged Hcrt nuclei (Wilcoxon rank-sum test, considering only those genes with a Bonferoni adjusted $P < 0.05$; statistical details are available in the supplementary text). (**D**) Volcano plot of regulation significance $-\text{Log}_{10}P$ against expression Log_2 fold change (FC) with expression level normalized to young dataset. (**E**) Percentage of Hcrt nuclei expressing *Kcnq* subtypes in young and aged female mice. Note the lower percentage of aged Hcrt nuclei actively expressing the dominant subtypes *Kcnq1/2/3/5*.

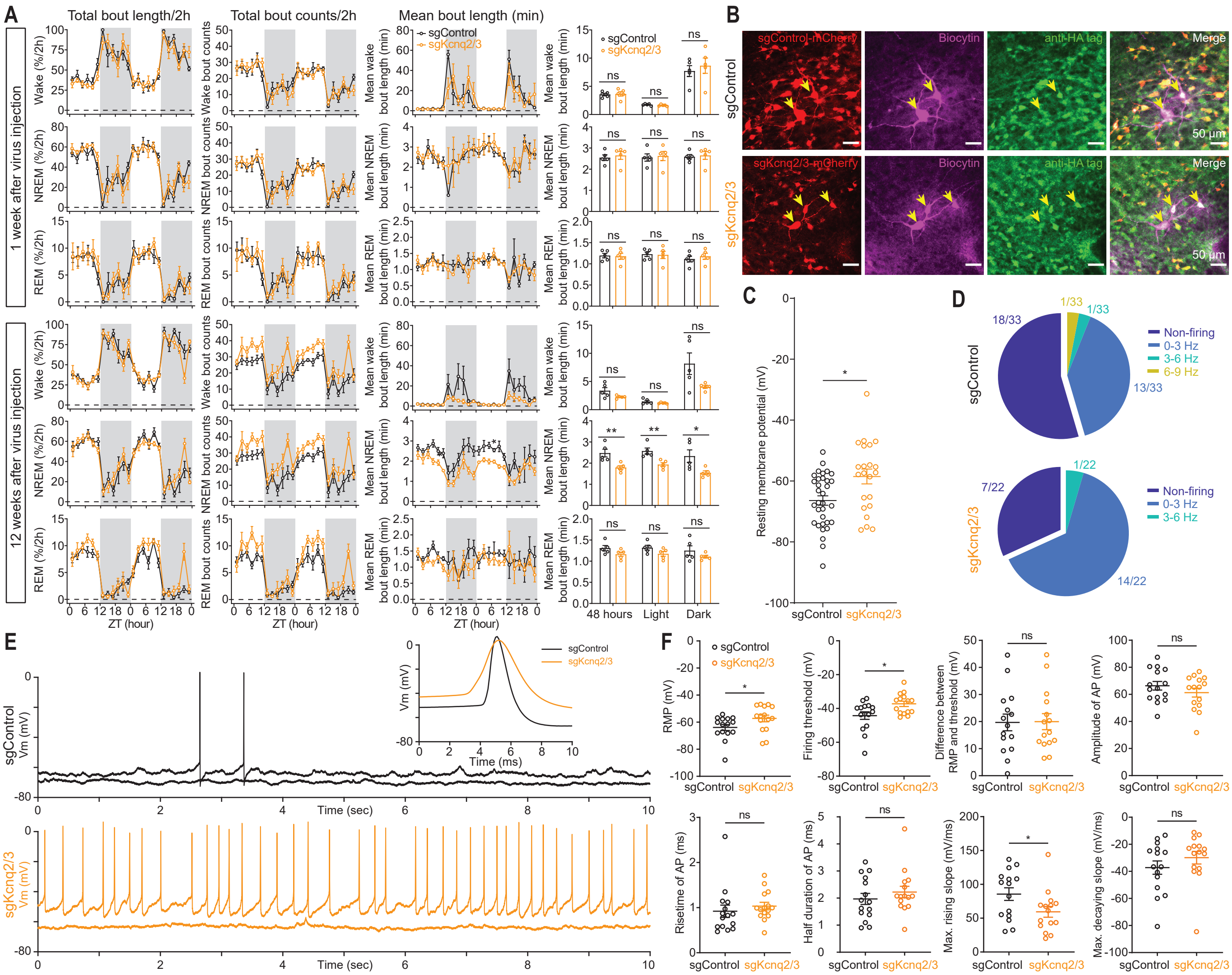

fig. S7. CRISPR/SaCas9-mediated disruption of *Kcnq2/3* genes in Hcrt neurons leads to NREM sleep fragmentation in young Hcrt::Cre mice. (**A**) 2 hour (left) binned percentage, (middle left) bout counts, (middle right) mean bout length, and (right) mean bout length based on circadian phase for wake, NREM, and REM sleep at 1 week (top), and 12 weeks (bottom) after injection of a virus mixture containing CRISPR reagents (n = 5 mice/group, dark phase indicated by gray shielding). (**B**) Images of representative slices from sgControl and sgKcnq2/3 groups infected with a virus mixture expressing fluorescent flag mCherry and HA tag following EEG-EMG recording at 12 weeks after virus injection. Patch clamp recorded cells were labeled with biocytin, and post hoc antibody staining against HA tag confirmed the cells expressing SaCas9 for data analyses. (**C**) Comparison of RMPs between sgControl and sgKcnq2/3 group (sgControl: n = 33 neurons from 6 mice versus sgKCNQ2/3: n = 22 neurons from 6 mice) pooled from 8 and 12 weeks after virus injection. (**D**) Fractions of neurons with different firing frequencies in the sgControl and sgKcnq2/3 group. (**E**) Representative traces with and without spontaneous firing activity. (Inset) Averaged traces for the young and aged spontaneous APs. (**F**) Comparisons of basic electrophysiological properties of neurons from the sgControl and sgKcnq2/3 group (sgControl: n = 15 neurons from 6 mice versus sgKCNQ2/3: n = 15 neurons from 6 mice). Data indicate mean ± SEM [(A) left to middle right, two-way RM ANOVA followed by Šidák's multiple comparisons; (A) right, Holm-Šidák; (C) and (F) Mann-Whitney *U* test; *P<0.05; statistical details are available in the supplementary text).

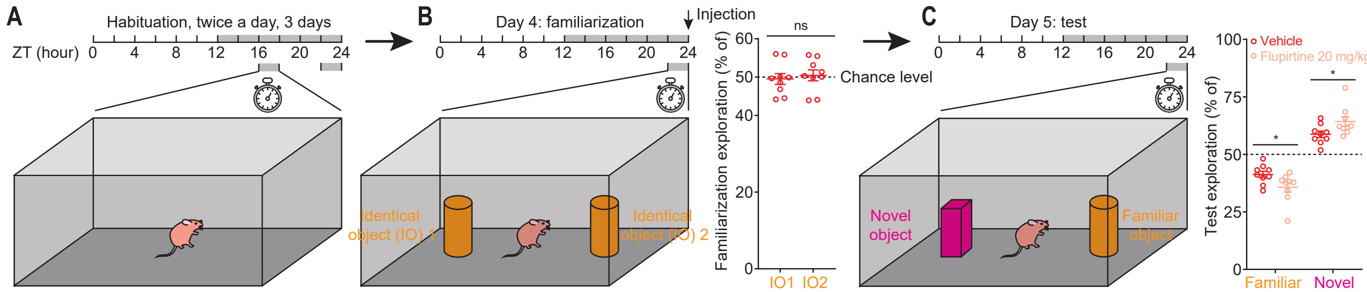

fig. S8. Performance of aged mice improved by flupirtine in an object recognition task. (**A**) Habituation session. (**B**) Familiarization session. (**C**) Test session. (A) to (C) n = 9 mice each group, unpaired *t*-test with Welch's correction, *$P < 0.05$; statistical details are available in the upplementary text.

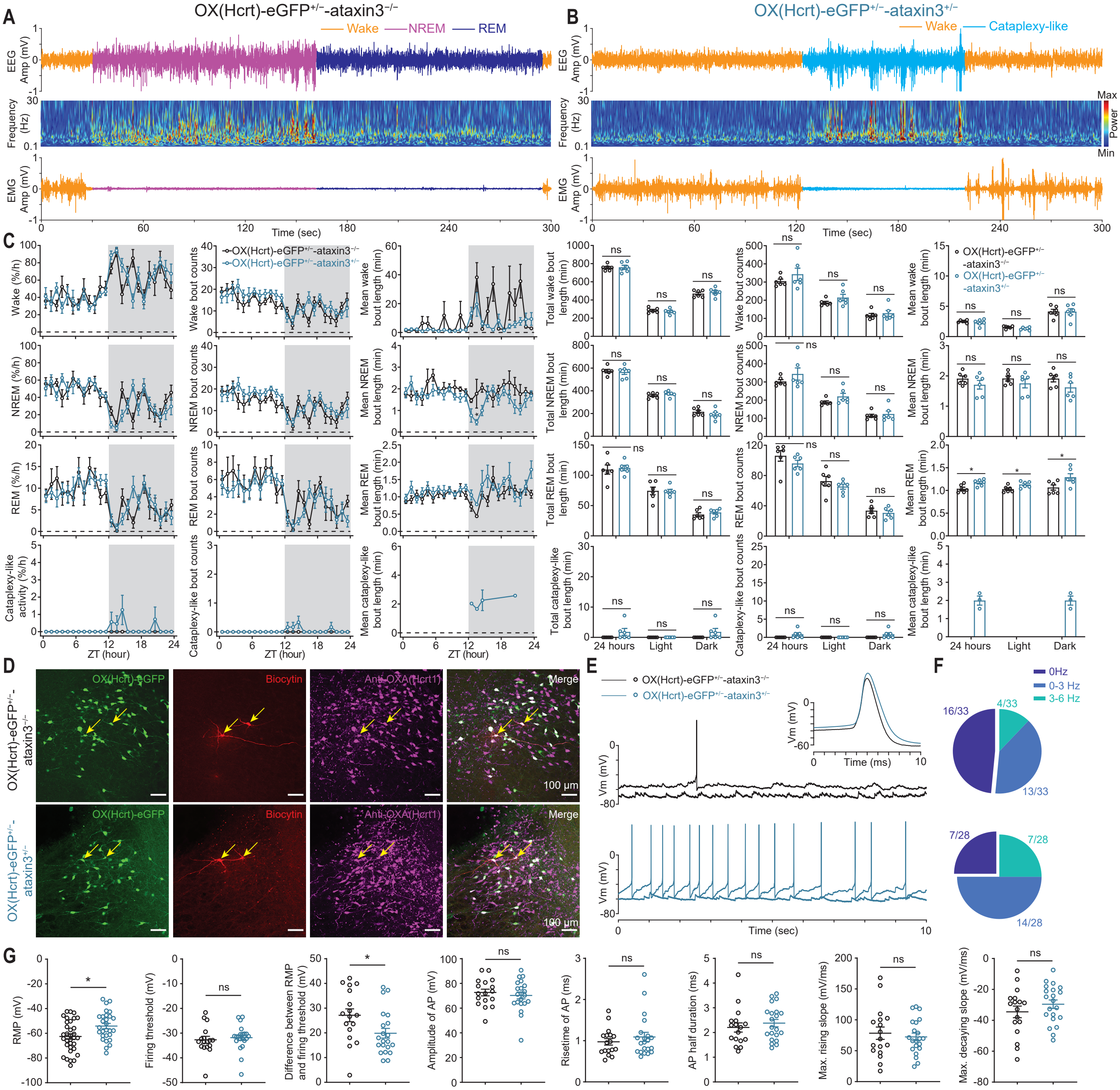

fig. S9. Cataplexy-like EEG-EMG pattern and NREM sleep fragmentation emerging during rapid OX(Hcrt) neuron loss in the OX(Hcrt)-ataxin3 narcolepsy mouse model at 5-week-old. (**A**) Representative EEG, EEG power spectrum, and EMG for a normal behavioral transition. (**B**) Representative EEG, EEG power spectrum, and EMG for a behavioral transition from wake to cataplexy-like EEG-EMG pattern. (**C**) Comparison of sleep architectures between OX(Hcrt)-eGFP$^{+/–}$-ataxin3$^{–/–}$ (control) and OX(Hcrt)-eGFP$^{+/–}$-ataxin3$^{+/–}$ (ataxin3^{+}) mice at 5-week-old. (**D**) Representative slices from control and ataxin3^{+} mice at 5-week-old. Patch clamp recorded cells labeled with biocytin and post hoc antibody staining against OXA(Hcrt1). (**E** to **G**) (E) Representative spontaneous activities (inset, averaged traces of the spontaneous APs) recorded from control and ataxin3^{+} mice, (F) fractions of neurons with different firing frequencies, and comparison of [first panel in (G)] RMPs (n = 33 neurons from three control mice versus n = 28 neurons from three ataxin3^{+} mice) and [other panels in (G)] other AP basic electrophysiological properties (n = 17 neurons from three control mice versus n = 21 neurons from three ataxin3^{+} mice) for spontaneously firing neurons. Statistical details are available in the supplementary text.

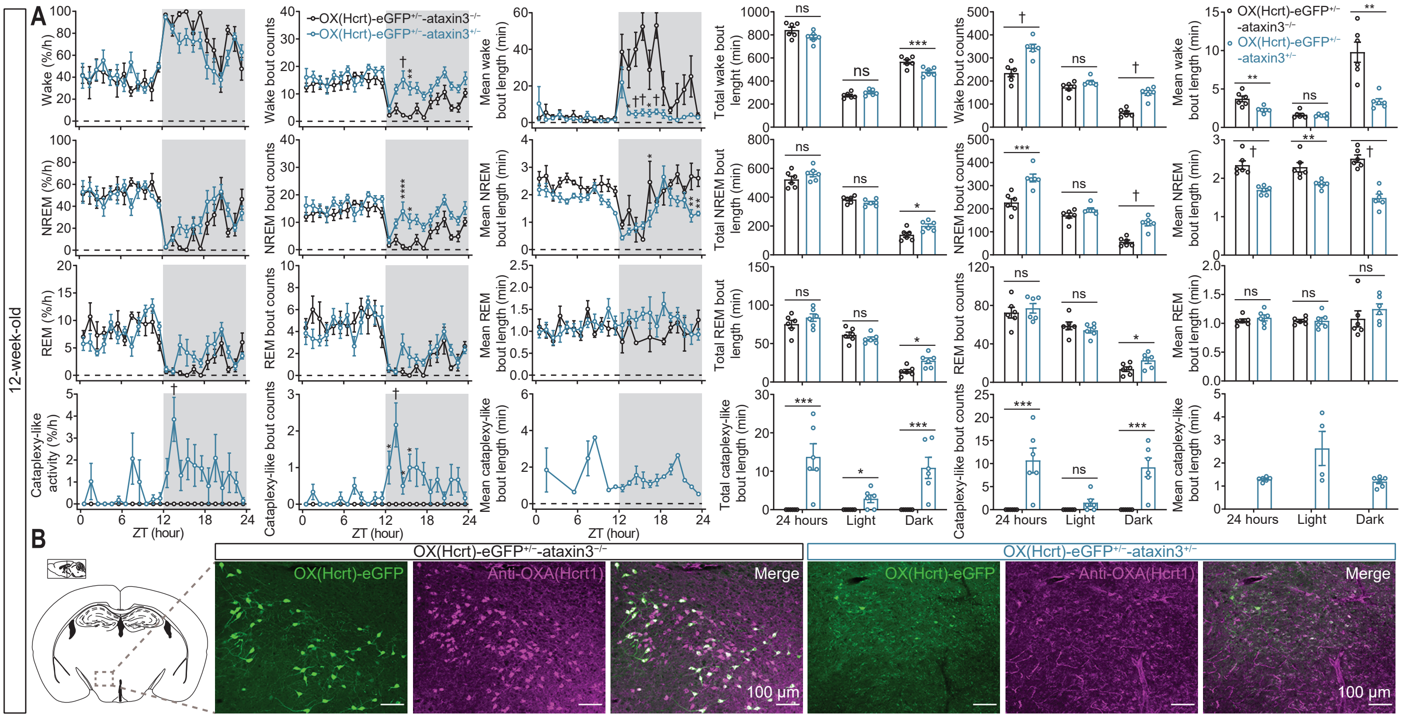

fig. S10. Cataplexy-like EEG-EMG pattern, and wake and NREM sleep fragmentation in the OX(Hcrt)-ataxin3 narcolepsy mouse model with a near complete OX(Hcrt) neuron loss at 12-week-old. (**A**) Comparison of sleep architectures between control and ataxin3^{+} mice at an age of 12 weeks. (**B**) Immunostaining against Hcrt1 revealed a near complete OX(Hcrt) neuron loss in the OX(Hcrt)-eGFP$^{+/-}$-ataxin3$^{+/-}$ group which displayed significant amount of cataplexy-like EEG-EMG activity at 12 weeks. Statistical details are available in the supplementary text.

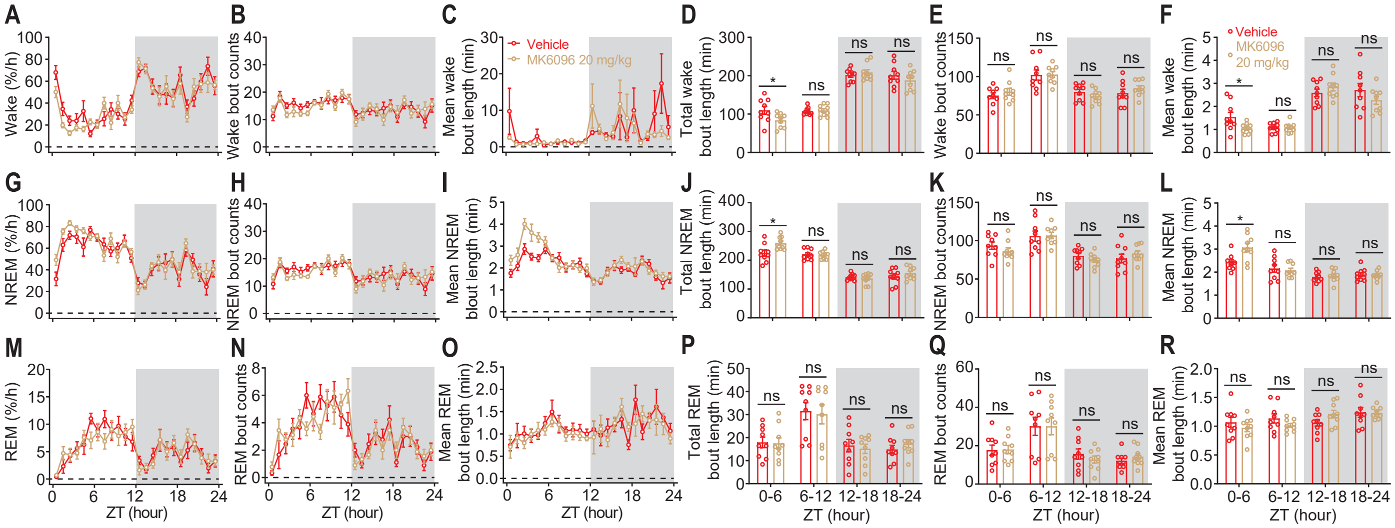

fig. S11. Effect of a dual Hcrt/OX receptor antagonist MK6096 (filorexant, 20 mg/kg) on sleep architecture in aged mice. (**A** to **F**) Comparison of (A) hourly-based percentage, (B) hourly-based bout counts, (C) hourly-based mean bout length, (D) total bout length, (E) total bout counts, and (F) mean bout length of wakefulness between vehicle- and MK6096-treated aged mice. (**G** to **L**) Comparison of (G) hourly-based percentage, (H) hourly-based bout counts, (I) hourly-based mean bout length, (J) total bout length, (K) total bout counts, and (L) mean bout length of NREM sleep between vehicle- and MK6096-treated aged mice. (**M** to **R**) Comparison of (M) hourly-based percentage, (N) hourly-based bout counts, (O) hourly-based mean bout length, (P) total bout length, (Q) total bout counts, and (R) mean bout length of REM sleep between vehicle- and MK6096-treated aged mice. Data indicate mean ± SEM [(A) to (C), (G) to (I), (M) to (O), two-way RM ANOVA (linear mixed-effects model) followed by Šidák's multiple comparisons, dark phase indicated by gray shielding; (D) to (F), (J) to (L), (P) to (R), Holm-Šidák; *$P < 0.05$, n = 9 mice each group; statistical details are available in the supplementary text].

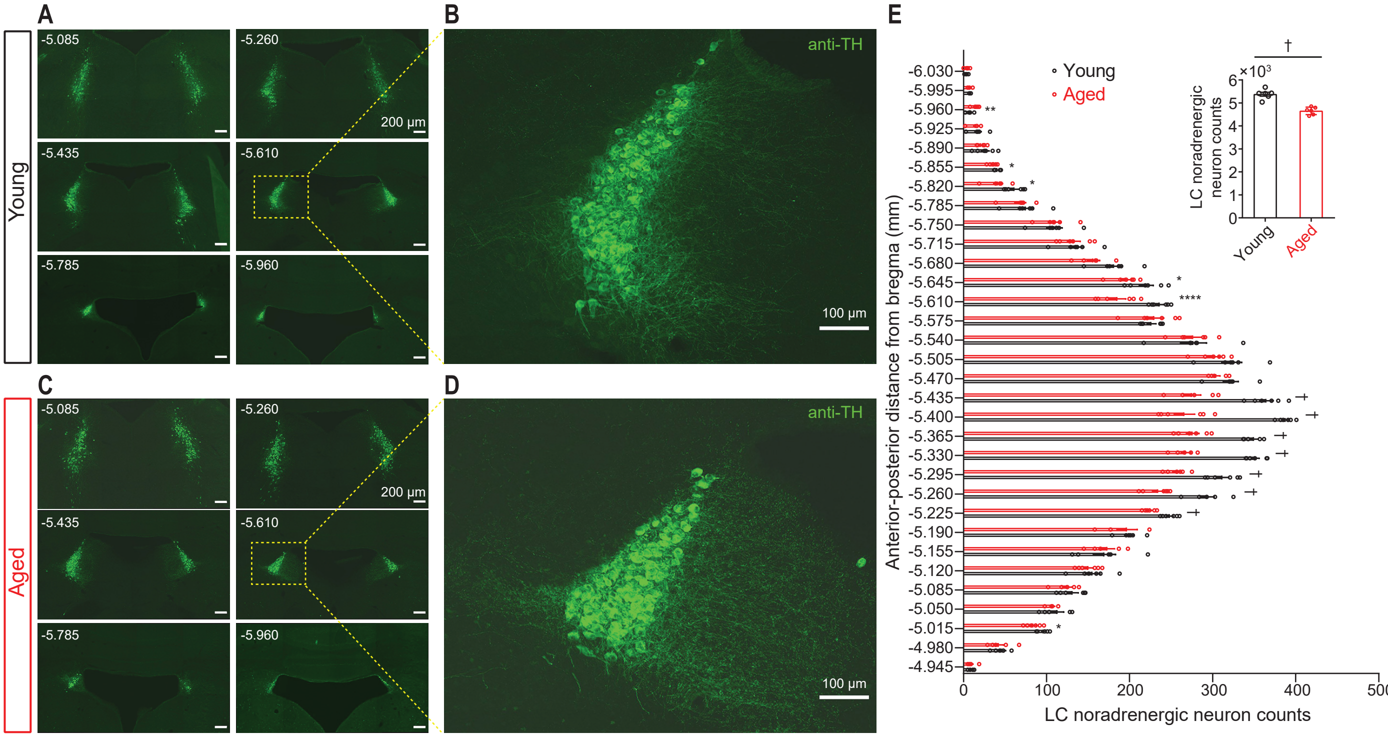

fig. S12. Locus coeruleus (LC) noradrenergic (NA) neuron loss in aged mice. (**A** and **B**) Antibody staining against tyrosine hydroxylase (TH) in brain slices spanning anterior-posterior (from bregma) – 4.945 to – 6.030 mm from a young mouse. (A) Representative young slices spaced by 0.175 mm, and (B) magnified display of the boxed region in panel A. (**C** and **D**) Antibody staining against TH in brain slices spanning anterior-posterior (from bregma) – 4.945 to – 6.030 mm from an aged mouse. (C) Representative aged slices spaced by 0.175 mm, and (D) magnified display of the boxed region in panel C. (**E**) Anterior-posterior location-matched comparison of noradrenergic neuron counts, and (inset) total noradrenergic neuron counts between the young and aged group. Data indicate mean ± SEM (n = 6 mice each group; two-way ANOVA followed by Šidák's multiple comparisons; inset: unpaired *t*-test; $*P < 0.05$, $**P < 0.01$, $****P < 0.001$, $\dagger P < 0.0005$; statistical details are available in the supplementary text).

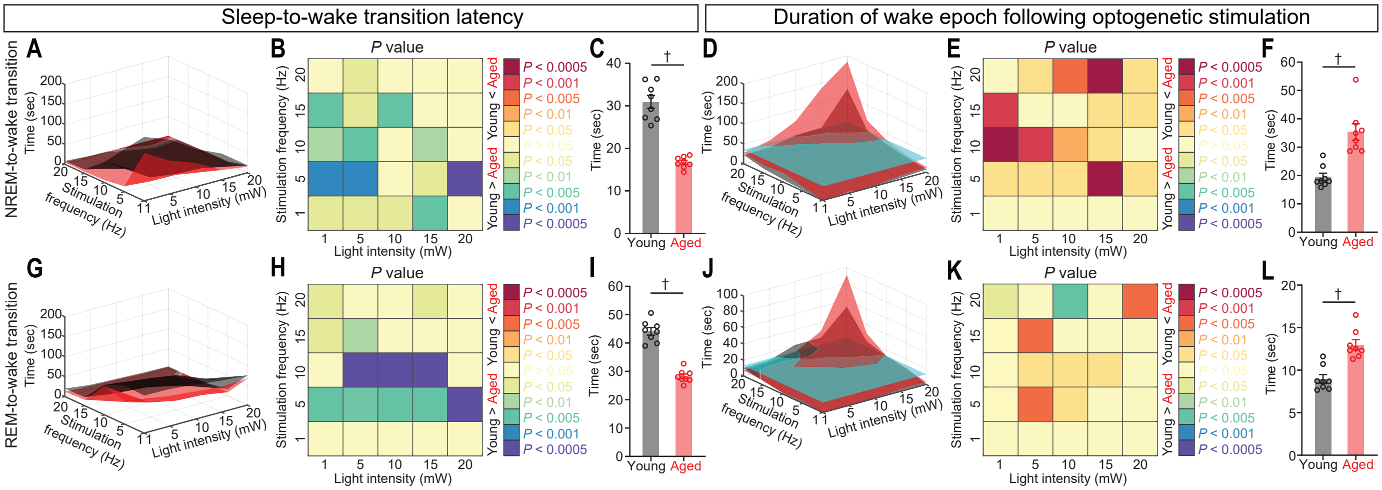

fig. S13. Longer wake bouts with shorter latencies upon optogenetic stimulation of LC NA neurons expressing ChR2-eYFP in aged TH::Cre mice. (**A**) Surface plot of NREM-to-wake transition latency based on the mean value of each stimulation condition. (**B** and **C**) Comparison of NREM-to-wake transition latency based on (B) each stimulation condition and (C) the mean value for each animal (C). (**D**) Surface plot of wake duration based on the mean value of each stimulation condition. The cyan cutaway surface indicates the mean value for the aged group. (**E** and **F**) Comparison of wake duration based on (E) each stimulation condition and (F) the mean value for each animal. (**G**) Surface plot of REM-to-wake transition latency based on the mean value of each stimulation condition. (**H** and **I**) Comparison of REM-to-wake transition latency based on (H) each stimulation condition and (I) the mean value for each animal. (**J**) Surface plot of wake duration based on the mean value of each stimulation condition. The cyan cutaway surface indicates the mean value for the aged group. (**K** and **L**) Comparison of wake duration based on (K) each stimulation condition and (L) the mean value for each animal. (B), (C), (E), (F), (H), (I), (K), (L): Mann-Whitney *U* test; †$P<0.0005$. Statistical details are available in the supplementary text.

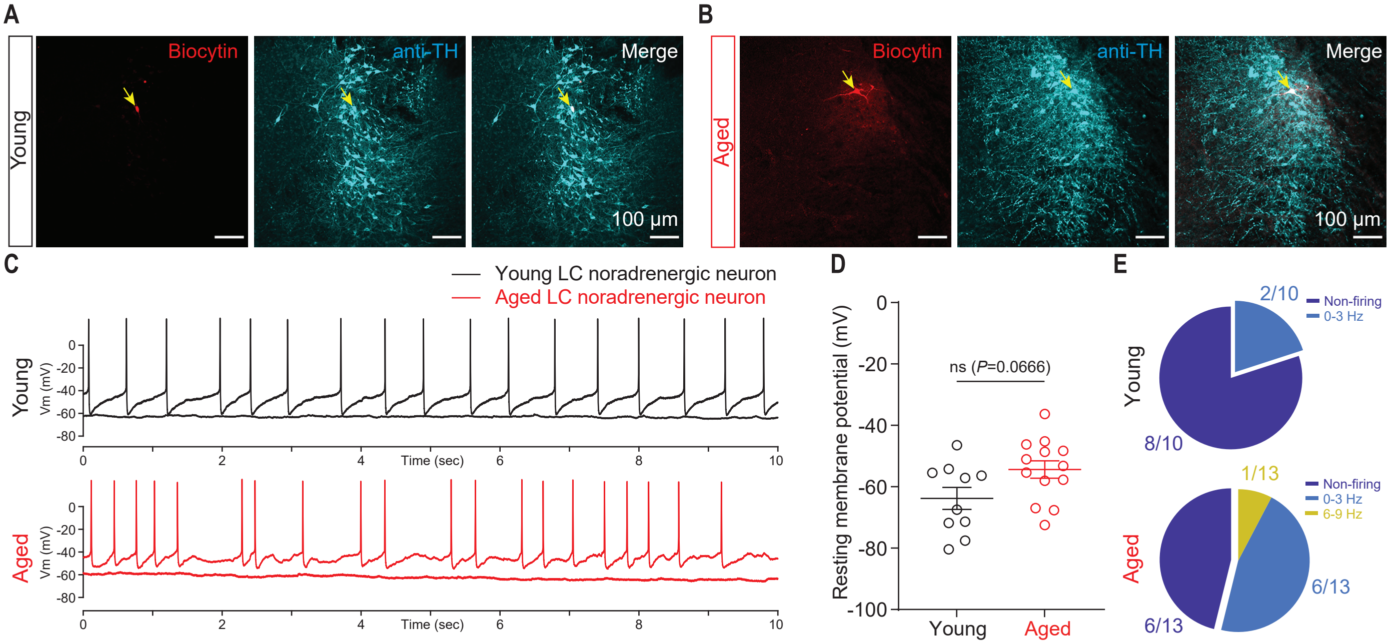

fig. S14. Higher spontaneous activity in aged LC NA neurons. (**A**) A representative slice from a young wild type mouse showing a patch clamp recorded neuron filled with biocytin and tyrosine hydroxylase (TH) antibody staining. (**B**) A representative slice from an aged wild type mouse showing a patch clamp recorded neuron filled with biocytin and TH antibody staining. (**C**) Representative recorded traces from (top) young and (bottom) aged LC NA neurons respectively. (**D**) Comparison of RMPs between young and aged LC NA neurons (Mann-Whitney *U* test; young: n = 10 neurons from three mice versus aged: n = 13 neurons from three mice). (**E**) Fractions of neurons with different firing frequencies for young and aged LC NA neurons. Only biocytin-labeled neurons co-stained with TH antibody were used for data analyses.

Supplementary Text

Details on statistical analyses

Statistical significance abbreviations: ns (not significant) *P*>0.05, **P*<0.05, ***P*<0.01, ****P*<0.005, *****P*<0.001, †*P*<0.0005.

MAIN FIGURES

Fig. 1

Panel	Data	Group size	Statistic method	Comparison	*P* value	Notation	F/t statistic
Fig. 1C. right middle	G^S transient peak	Young: n=128 vs. Aged: n=171	Unpaired *t*-test with Welch's correction	Young versus (vs.) Aged	<0.0001	†	t=10.59
	G^S transient duration	Young: n=128 vs. Aged: n=171	Unpaired *t*-test with Welch's correction	Young vs. Aged	<0.0001	†	t=6.913
Fig. 1C. right bottom left	G^S Z score	n=6/group	Unpaired t-test with Welch's correction	Young vs. Aged	0.0022	***	t=4.293
Fig. 1C. right bottom right	G^S transient frequency	n=6/group	Unpaired *t*-test with Welch's correction	Young vs. Aged	0.0612	ns	t=2.161
Fig. 1D right middle	G^W epoch peak	Young: n=102 vs. Aged: n=137	Unpaired *t*-test with Welch's correction	Young vs. Aged	<0.0001	†	t=6.357
	G^W epoch duration	Young: n=102 vs. Aged: n=137	Unpaired *t*-test with Welch's correction	Young vs. Aged	0.0061	**	t=2.787
Fig. 1D. right bottom left	G^W Z score	n=6/group	Unpaired *t*-test with Welch's correction	Young vs. Aged	0.0196	*	t=2.852
Fig. 1D. right bottom right	G^W transient frequency	n=6/group	Unpaired *t*-test with Welch's correction	Young vs. Aged	0.0035	***	t=4.286
Fig. 1E	Animal-based averaged duration of, sleep, wake, S-W episode	n=6/group	Unpaired *t*-test with Welch's correction	Sleep Y vs. A	0.0328	*	t=2.504
				Wake Y vs. A	0.0110	*	t=3.151
				S-W episode Y vs. A	0.0007	****	t=5.911
Fig. 1F. G^W epoch count/h against mean sleep bout duration	Young	n=6/group	Pearson correlation, linear fit	Slope vs. zero	0.2764	ns	F=1.586
	Aged	n=6/group		Slope vs. zero	0.0372	*	F=9.447
	Pooled	n=6/group		Slope vs. zero	0.0015	***	F=18.70

Fig. 2

Panel	Data	Group size	Statistic method	Comparison condition	*P* value	Notation	F/t statistic
Fig. 2B	Latency for NREM-to-wake transition across stimulation parameters: Young vs. Aged	n=8 mice each group	Mann-Whitney *U* test	1 mW, 1 Hz	0.39782	ns	N/A
				1 mW, 5 Hz	0.00047	†	N/A
				1 mW, 10 Hz	0.00404	***	N/A
				1 mW, 15 Hz	0.00995	**	N/A
				1 mW, 20 Hz	0.00917	**	N/A
				5 mW, 1 Hz	0.00016	†	N/A
				5 mW, 5 Hz	0.00016	†	N/A
				5 mW, 10 Hz	0.00031	†	N/A
				5 mW, 15 Hz	0.00047	†	N/A
				5 mW, 20 Hz	0.01772	*	N/A
				10 mW, 1 Hz	0.00062	****	N/A
				10 mW, 5 Hz	0.00870	**	N/A
				10 mW, 10 Hz	0.42735	ns	N/A
				10 mW, 15 Hz	0.17591	ns	N/A
				10 mW, 20 Hz	0.00016	†	N/A

				15 mW, 1 Hz	0.00311	***	N/A
				15 mW, 5 Hz	0.01103	*	N/A
				15 mW, 10 Hz	0.42346	ns	N/A
				15 mW, 15 Hz	0.05252	ns	N/A
				15 mW, 20 Hz	0.00016	†	N/A
				20 mW, 1 Hz	0.00016	†	N/A
				20 mW, 5 Hz	0.08500	ns	N/A
				20 mW, 10 Hz	0.00016	†	N/A
				20 mW, 15 Hz	0.00016	†	N/A
				20 mW, 20 Hz	0.00031	†	N/A
Fig. 2C	Data in panel B aggregated for individual animal	n=8 mice each group	Mann-Whitney *U* test	Young vs. Aged	0.10490	ns	N/A
Fig. 2E	Wake duration following optogenetic stimulation during NREM sleep across stimulation parameters: Young vs. Aged	n=8 mice each group	Mann-Whitney *U* test	1 mW, 1 Hz	0.38928	ns	N/A
				1 mW, 5 Hz	0.00016	†	N/A
				1 mW, 10 Hz	0.00016	†	N/A
				1 mW, 15 Hz	0.00016	†	N/A
				1 mW, 20 Hz	0.00062	****	N/A
				5 mW, 1 Hz	0.02999	*	N/A
				5 mW, 5 Hz	0.00031	†	N/A
				5 mW, 10 Hz	0.57374	ns	N/A
				5 mW, 15 Hz	0.09883	ns	N/A
				5 mW, 20 Hz	0.13038	ns	N/A
				10 mW, 1 Hz	0.00062	****	N/A
				10 mW, 5 Hz	0.04988	*	N/A
				10 mW, 10 Hz	0.00699	**	N/A
				10 mW, 15 Hz	0.00031	†	N/A
				10 mW, 20 Hz	0.00295	***	N/A
				15 mW, 1 Hz	0.00062	****	N/A
				15 mW, 5 Hz	0.03015	*	N/A
				15 mW, 10 Hz	0.01476	*	N/A
				15 mW, 15 Hz	0.00016	†	N/A
				15 mW, 20 Hz	0.04056	*	N/A
				20 mW, 1 Hz	0.00031	†	N/A
				20 mW, 5 Hz	0.00124	***	N/A
				20 mW, 10 Hz	0.00124	***	N/A
				20 mW, 15 Hz	0.01476	*	N/A
				20 mW, 20 Hz	0.02067	*	N/A
Fig. 2F	Data in panel E aggregated for individual animal	n=8 mice each group	Mann-Whitney *U* test	Young vs. Aged	0.00020	†	N/A
Fig. 2H	Latency for REM-to-wake transition across stimulation parameters: Young vs. Aged	n=8 mice each group	Mann-Whitney *U* test	1 mW, 1 Hz	0.98135	ns	N/A
				1 mW, 5 Hz	0.00373	***	N/A
				1 mW, 10 Hz	0.45082	ns	N/A
				1 mW, 15 Hz	0.43761	ns	N/A
				1 mW, 20 Hz	0.14126	ns	N/A
				5 mW, 1 Hz	0.00016	†	N/A
				5 mW, 5 Hz	0.00016	†	N/A
				5 mW, 10 Hz	0.00342	***	N/A
				5 mW, 15 Hz	0.00249	***	N/A
				5 mW, 20 Hz	0.00016	†	N/A
				10 mW, 1 Hz	0.00016	†	N/A
				10 mW, 5 Hz	0.00218	***	N/A
				10 mW, 10 Hz	0.01243	*	N/A
				10 mW, 15 Hz	0.05284	ns	N/A
				10 mW, 20 Hz	0.00016	†	N/A
				15 mW, 1 Hz	0.01927	*	N/A

				15 mW, 5 Hz	0.05221	ns	N/A
				15 mW, 10 Hz	0.07397	ns	N/A
				15 mW, 15 Hz	0.01445	*	N/A
				15 mW, 20 Hz	0.00218	†	N/A
				20 mW, 1 Hz	0.00016	***	N/A
				20 mW, 5 Hz	0.07280	ns	N/A
				20 mW, 10 Hz	0.59036	ns	N/A
				20 mW, 15 Hz	0.00093	****	N/A
				20 mW, 20 Hz	0.00171	***	N/A
Fig. 2I	Data in panel H aggregated for individual animal	n=8 mice each group	Mann-Whitney *U* test	Young vs. Aged	0.00470	***	N/A
Fig. 2K	Wake duration following optogenetic stimulation during REM sleep across stimulation parameters: Young vs. Aged	n=8 mice each group	Mann-Whitney *U* test	1 mW, 1 Hz	0.56923	ns	N/A
				1 mW, 5 Hz	0.00016	†	N/A
				1 mW, 10 Hz	0.00016	†	N/A
				1 mW, 15 Hz	0.01041	*	N/A
				1 mW, 20 Hz	0.00016	†	N/A
				5 mW, 1 Hz	0.00948	**	N/A
				5 mW, 5 Hz	0.00016	†	N/A
				5 mW, 10 Hz	0.00047	†	N/A
				5 mW, 15 Hz	0.00047	†	N/A
				5 mW, 20 Hz	0.00016	†	N/A
				10 mW, 1 Hz	0.02191	*	N/A
				10 mW, 5 Hz	0.00186	***	N/A
				10 mW, 10 Hz	0.00016	†	N/A
				10 mW, 15 Hz	0.00420	***	N/A
				10 mW, 20 Hz	0.01041	*	N/A
				15 mW, 1 Hz	0.00031	†	N/A
				15 mW, 5 Hz	0.00016	†	N/A
				15 mW, 10 Hz	0.05315	ns	N/A
				15 mW, 15 Hz	0.01041	*	N/A
				15 mW, 20 Hz	0.00016	†	N/A
				20 mW, 1 Hz	0.00016	†	N/A
				20 mW, 5 Hz	0.00016	†	N/A
				20 mW, 10 Hz	0.00295	***	N/A
				20 mW, 15 Hz	0.00016	†	N/A
				20 mW, 20 Hz	0.00109	***	N/A
Fig. 2L	Data in panel K aggregated for individual animal	n=8 mice each group	Mann-Whitney *U* test	Young vs. Aged	0.00020	†	N/A

Fig. 3

Panel	**Data**	**Group size**	**Statistic method**	**Comparison**	***P* value**	**Notation**	**F/t statistic**
Fig. 3D	Input resistance	Young: n=33 Aged: n=21	Mann-Whitney *U* test	Young vs. Aged	0.4488	ns	N/A
Fig. 3E	Resting membrane potential	Young: n=33 Aged: n=21	Mann-Whitney *U* test	Young vs. Aged	0.0165	*	N/A
Fig. 3F	Firing threshold	Young: n=12 Aged: n=9	Mann-Whitney *U* test	Young vs. Aged	0.5660	ns	N/A
Fig. 3G	Difference between RMP and threshold	Young: n=12 Aged: n=9	Mann-Whitney *U* test	Young vs. Aged	0.0056	**	N/A
Fig. 3H	Amplitude of AP	Young: n=12 Aged: n=9	Mann-Whitney *U* test	Young vs. Aged	0.0339	*	N/A
Fig. 3I	Risetime of AP	Young: n=12 Aged: n=9	Mann-Whitney *U* test	Young vs. Aged	0.2773	ns	N/A
Fig. 3J	Half duration of AP	Young: n=12 Aged: n=9	Mann-Whitney *U* test	Young vs. Aged	0.5538	ns	N/A

Fig. 3K	Max. rising slope	Young: n=12 Aged: n=9	Mann-Whitney *U* test	Young vs. Aged	0.1694	ns	N/A
Fig. 3L	Max. decaying slope	Young: n=12 Aged: n=9	Mann-Whitney *U* test	Young vs. Aged	0.3544	ns	N/A
Fig. 3N	Response attenuation upon optogenetic stimulations	Young: n=23 Aged: n=21	Two-way ANOVA	Stimulation frequency	<0.0001	†	$F_{(4, 206)}$=32.18
				Age	<0.0001	†	$F_{(1, 206)}$=17.69
				Interaction	0.8059	ns	$F_{(4, 206)}$=0.8059
			Post-hoc Šidák's multiple comparisons	1 Hz	0.9728	ns	t=0.6541
				5 Hz	0.3049	ns	t=1.820
				10 Hz	0.0158	*	t=2.985
				15 Hz	0.0638	ns	t=2.503
				20 Hz	0.5438	ns	t=1.462
Fig. 3O	Spikelets upon step current injection	Young: n=33 Aged: n=26	Two-way ANOVA	Current	<0.0001	†	$F_{(7, 454)}$=15.09
				Age	<0.0001	†	$F_{(1, 454)}$=26.41
				Interaction	0.1413	ns	$F_{(7, 454)}$=1.573
			Post-hoc Šidák's multiple comparisons	-50 pA	>0.9999	ns	t=0.03566
				0 pA	>0.9999	ns	t=0.3015
				50 pA	0.6762	ns	t=1.511
				100 pA	0.0344	*	t=2.865
				150 pA	0.0242	*	t=2.978
				200 pA	0.0176	*	t=3.077
				250 pA	0.0488	*	t=2.748
				300 pA	0.9427	ns	t=1.037

Fig. 4

Panel	Data	Group size	Statistic method	Comparison	*P* value	Notation	F/q statistic
Fig. 4B	Resting membrane potential	n=19	Wilcoxon matched-pairs signed rank test	ACSF vs. XE991	0.0012	***	N/A
Fig. 4C	Firing rate	n=19	Wilcoxon matched-pairs signed rank test	ACSF vs. XE991	0.0078	**	N/A
Fig. 4E	Resting membrane potential	n=8	RM one-way ANOVA	Across treatments	<0.0001	†	F=64.13
			Post-hoc Tukey's multiple comparisons	ACSF vs. solvent	0.0509	ns	q=4.146
				ACSF vs. Flup	<0.0001	†	q=14.65
				Solvent vs. Flup	0.0006	****	q=9.597
Fig. 4F	Firing rate	n=8	RM one-way ANOVA	Across treatments	0.0072	**	F=11.82
			Post-hoc Tukey's multiple comparisons	ACSF vs. solvent	0.0725	ns	q=3.781
				ACSF vs. Flup	0.0210	*	q=5.087
				Solvent vs. Flup	0.0294	*	q=4.724
Fig. 4G. right top	Young Hcrt M current	n=6	Paired *t*-test	Before vs. after XE991	0.0048	***	t=4.824
Fig. 4G. right bottom	Young Hcrt M current	n=10	Paired *t*-test	Before vs. after Flupirtine	0.0409	*	t=2.385
Fig. 4H. right top	Aged Hcrt M current	n=7	Paired *t*-test	Before vs. after XE991	0.1799	ns	t=1.518
Fig. 4H. right bottom	Aged Hcrt M current	n=15	Paired *t*-test	Before vs. after Flupirtine	0.0002	†	t=4.981
Fig. 4I	Basal M current	Y: n=25 A: n=26	Unpaired *t*-test with Welch's correction	Young vs. Aged	0.0403	*	t=2.123
Fig. 4J. right	KCNQ2 quantification	n=4 each group	Paired *t*-test	Young vs. Aged	0.0495	*	t=3.196

Fig. 5

Panel	Data	Group size	Statistic method	Comparison	*P* value	Notation	F/t statistic
Fig. 5B. Week1 top panel 1	Wake amount/2h	n=10 each group	Two-way RM ANOVA, Post-hoc Šidák	Main effect of group	0.6969	ns	$F_{(1, 18)}$= 0.1567
Fig. 5B. Week1 top panel 2	Wake bout count/2h	n=10 each group	Two-way RM ANOVA, Post-hoc Šidák	Main effect of group	0.8736	ns	$F_{(1, 18)}$= 0.02606
Fig. 5B. Week1 top panel 3	Mean wake bout length	n=10 each group	Two-way RM ANOVA, Post-hoc Šidák	Main effect of group	0.4600	ns	$F_{(1, 18)}$= 0.5701
Fig. 5B. Week1 top panel 4	Mean wake bout length	n=10 each group	Holm-Šidák	48 hour	0.8668	ns	t=0.1702
				Light	0.6553	ns	t=0.4539
				Dark	0.7029	ns	t=0.3880
Fig. 5B. Week1 middle panel 1	NREM amount/2h	n=10 each group	Two-way RM ANOVA, Post-hoc Šidák	Main effect of group	0.7216	ns	$F_{(1, 18)}$= 0.1311
Fig. 5B. Week1 middle panel 2	NREM bout count/2h	n=10 each group	Two-way RM ANOVA, Post-hoc Šidák	Main effect of group	0.8840	ns	$F_{(1, 18)}$= 0.02191
Fig. 5B. Week1 middle panel 3	Mean NREM bout length	n=10 each group	Two-way RM ANOVA, Post-hoc Šidák	Main effect of group	0.7202	ns	$F_{(1, 18)}$= 0.1324
Fig. 5B. Week1 middle panel 4	Mean NREM bout length	n=10 each group	Holm-Šidák	48 hour	0.6962	ns	t=0.3968
				Light	0.7366	ns	t=0.3416
				Dark	0.9847	ns	t=0.01948
Fig. 5B. Week1 bottom panel 1	REM amount/2h	n=10 each group	Two-way RM ANOVA, Post-hoc Šidák	Main effect of group	0.8387	ns	$F_{(1, 18)}$= 0.04263
Fig. 5B. Week1 bottom panel 2	REM bout count/2h	n=10 each group	Two-way RM ANOVA, Post-hoc Šidák	Main effect of group	0.8594	ns	$F_{(1, 18)}$= 0.03229
Fig. 5B. Week1 bottom panel 3	Mean REM bout length	n=10 each group	Two-way RM ANOVA, Post-hoc Šidák	Main effect of group	0.9519	ns	$F_{(1, 18)}$= 0.003740
Fig. 5B. Week1 bottom panel 4	Mean REM bout length	n=10 each group	Holm-Šidák	48 hour	0.9471	ns	t=0.06733
				Light	0.8476	ns	t=0.1950
				Dark	0.8366	ns	t=0.2093
Fig. 5B. Week8 top panel 1	Wake amount/2h	n=10 each group	Two-way RM ANOVA, Post-hoc Šidák	Main effect of group	0.6385	ns	$F_{(1, 18)}$= 0.2283
Fig. 5B. Week8 top panel 2	Wake bout count/2h	n=10 each group	Two-way RM ANOVA, Post-hoc Šidák	Main effect of group	0.0019	***	$F_{(1, 18)}$=13.16
Fig. 5B. Week8 top panel 3	Mean wake bout length	n=10 each group	Two-way RM ANOVA, Post-hoc Šidák	Main effect of group	0.5679	ns	$F_{(1, 18)}$= 0.3386
Fig. 5B. Week8 top panel 4	Mean wake bout length	n=10 each group	Holm-Šidák	48 hour	0.04055	*	t=2.207
				Light	0.1274	ns	t=1.598
				Dark	0.1068	ns	t=1.698
Fig. 5B. Week8 middle panel 1	NREM amount/2h	n=10 each group	Two-way RM ANOVA, Post-hoc Šidák	Main effect of group	0.5398	ns	$F_{(1, 18)}$= 0.3907
Fig. 5B. Week8 middle panel 2	NREM bout count/2h	n=10 each group	Two-way RM ANOVA, Post-hoc Šidák	Main effect of group	0.0030	***	$F_{(1, 18)}$=11.74
Fig. 5B. Week8 middle panel 3	Mean NREM bout length	n=10 each group	Two-way RM ANOVA, Post-hoc Šidák	Main effect of group	<0.0001	†	$F_{(1, 18)}$=37.29
Fig. 5B. Week8 middle panel 4	Mean NREM bout length	n=10 each group	Holm-Šidák	48 hour	<0.0001	†	t=5.085
				Light	0.000157	†	t=4.760
				Dark	0.002341	***	t=3.540
Fig. 5B. Week8 bottom panel 1	REM amount/2h	n=10 each group	Two-way RM ANOVA, Post-hoc Šidák	Main effect of group	0.6737	ns	$F_{(1, 18)}$= 0.1833
Fig. 5B. Week8 bottom panel 2	REM bout count/2h	n=10 each group	Two-way RM ANOVA, Post-hoc Šidák	Main effect of group	0.3055	ns	$F_{(1, 18)}$=1.112
Fig. 5B. Week8 bottom panel 3	Mean REM bout length	n=10 each group	Two-way RM ANOVA, Post-hoc Šidák	Main effect of group	0.7868	ns	$F_{(1, 18)}$= 0.07540
Fig. 5B. Week8 bottom panel 4	Mean REM bout length	n=10 each group	Holm-Šidák	48 hour	0.1716	ns	t=1.424
				Light	0.1061	ns	t=1.701
				Dark	0.8467	ns	t=0.1961
Fig. 5D	RMP	n=14 each group	Mann-Whitney *U* test	sgControl vs. sgKcnq2/3	0.0122	*	N/A

Fig. 6

Panel	Data	Group size	Statistic method	Comparison	*P* value	Notation	F/t statistic
Fig. 6A. Row1 Panel 1	Wake quantification in young mice	n=7	Two-way mixed effects model, Post-hoc Šidák	Time	<0.0001	†	$F_{(23, 276)}$=17.15
				Treatment	0.8333	ns	$F_{(1, 12)}$=0.04628
				Interaction	0.5378	ns	$F_{(23, 276)}$=0.9452
Fig. 6A. Row1 Panel 2	NREM quantification in young mice	n=7	Two-way mixed effects model, Post-hoc Šidák	Time	<0.0001	†	$F_{(23, 276)}$=16.21
				Treatment	0.8143	ns	$F_{(1, 12)}$=0.05762
				Interaction	0.5191	ns	$F_{(23, 276)}$=0.9591
Fig. 6A. Row1 Panel 3	REM quantification in young mice	n=7	Two-way mixed effects model, Post-hoc Šidák	Time	<0.0001	†	$F_{(23, 276)}$=15.15
				Treatment	0.7977	ns	$F_{(1, 12)}$=0.06867
				Interaction	0.5437	ns	$F_{(23, 276)}$=0.9408
Fig. 6A. Row2 Panel 1	Wake bout count in young mice	n=7	Two-way mixed effects model, Post-hoc Šidák	Time	<0.0001	†	$F_{(23, 276)}$=10.34
				Treatment	0.8007	ns	$F_{(1, 12)}$=0.06662
				Interaction	0.6752	ns	$F_{(23, 276)}$=0.8431
Fig. 6A. Row2 Panel 2	NREM bout count in young mice	n=7	Two-way mixed effects model, Post-hoc Šidák	Time	0.0001	†	$F_{(23, 276)}$=11.28
				Treatment	0.7160	ns	$F_{(1, 12)}$=0.1388
				Interaction	0.6661	ns	$F_{(23, 276)}$=0.8500
Fig. 6A. Row2 Panel 3	REM bout count in young mice	n=7	Two-way mixed effects model, Post-hoc Šidák	Time	<0.0001	†	$F_{(23, 276)}$=13.85
				Treatment	0.3511	ns	$F_{(1, 12)}$=0.9413
				Interaction	0.0734	ns	$F_{(23, 276)}$=1.488
Fig. 6A. Row3 Panel 1	Mean wake bout length in young mice	n=7	Two-way mixed effects model, Post-hoc Šidák	Time	<0.0001	†	$F_{(23, 230)}$=7.920
				Treatment	0.9289	ns	$F_{(1, 12)}$=0.008296
				Interaction	0.8540	ns	$F_{(23, 276)}$=0.6909
Fig. 6A. Row3 Panel 2	Mean NREM bout length in young mice	n=7	Two-way mixed effects model, Post-hoc Šidák	Time	0.0011	***	$F_{(23, 260)}$=4.613
				Treatment	0.6774	ns	$F_{(1, 12)}$=0.1735
				Interaction	0.4456	ns	$F_{(23, 260)}$= 1.016
Fig. 6A. Row3 Panel 3	Mean REM bout length in young mice	n=7	Two-way mixed effects model, Post-hoc Šidák	Time	0.0643	ns	$F_{(23, 180)}$=1.534
				Treatment	0.2584	ns	$F_{(1, 12)}$=1.408
				Interaction	0.0168	*	$F_{(23, 180)}$=1.814
Fig. 6B. Row1 Panel 1	Wake quantification in aged mice	n=6	Two-way mixed effects model, Post-hoc Šidák	Time	<0.0001	†	$F_{(23, 230)}$=10.48
				Treatment	0.3343	ns	$F_{(1, 10)}$=1.029
				Interaction	0.7784	ns	$F_{(23, 230)}$=0.7601
Fig. 6B. Row1 Panel 2	NREM quantification in aged mice	n=6	Two-way mixed effects model, Post-hoc Šidák	Time	<0.0001	†	$F_{(23, 230)}$=9.977
				Treatment	0.2593	ns	$F_{(1, 10)}$=1.430
				Interaction	0.7492	ns	$F_{(23, 230)}$=0.7845
Fig. 6B. Row1 Panel 3	REM quantification in aged mice	n=6	Two-way mixed effects model, Post-hoc Šidák	Time	<0.0001	†	$F_{(23, 230)}$=10.66
				Treatment	0.7245	ns	$F_{(1, 10)}$=0.1315
				Interaction	0.1686	ns	$F_{(23, 230)}$=1.300
Fig. 6B. Row2 Panel 1	Wake bout count in aged mice	n=6	Two-way mixed effects model, Post-hoc Šidák	Time	0.0011	***	$F_{(23, 230)}$=4.036
				Treatment	0.1616	ns	$F_{(1, 10)}$ =2.285
				Interaction	0.1602	ns	$F_{(23, 230)}$=1.312
Fig. 6B. Row2 Panel 2	NREM bout count in aged mice	n=6	Two-way mixed effects model, Post-hoc Šidák	Time	0.0003	†	$F_{(23, 230)}$=4.660
				Treatment	0.1571	ns	$F_{(1, 10)}$ =2.339
				Interaction	0.1959	ns	$F_{(23, 230)}$=1.261
Fig. 6B. Row3 Panel 3	REM bout count in aged mice	n=6	Two-way mixed effects model, Post-hoc Šidák	Time	<0.0001	†	$F_{(23, 230)}$=9.518
				Treatment	0.5511	ns	$F_{(1, 10)}$=0.3806
				Interaction	0.0746	ns	$F_{(23, 230)}$=1.491
Fig. 6B. Row3 Panel 1	Mean wake bout length in aged mice	n=6	Two-way mixed effects model, Post-hoc Šidák	Time	0.0337	*	$F_{(23, 230)}$=2.809
				Treatment	0.8607	ns	$F_{(1, 10)}$=0.03240
				Interaction	0.9615	ns	$F_{(23, 230)}$=0.5350
Fig. 6B. Row3 Panel 2	Mean NREM bout length in aged mice	n=6	Two-way mixed effects model, Post-hoc Šidák	Time	0.0005	****	$F_{(23, 230)}$=4.820
				Treatment	0.0200	*	$F_{(1, 10)}$=7.636
				Interaction	<0.0001	†	$F_{(23, 228)}$=3.639
Fig. 6B. Row3 Panel 2	Mean REM bout length in aged mice	n=6	Two-way mixed effects model, Post-hoc Šidák	Time	0.4123	ns	$F_{(23, 181)}$=1.020
				Treatment	0.6743	ns	$F_{(1, 10)}$=0.1873
				Interaction	0.7244	ns	$F_{(23, 181)}$=0.8034
Fig. 6G. left	Band power	n=7	Holm-Šidák	Delta	0.6307	ns	t=0.4937

				Theta	0.7331	ns	t=0.3491
Fig. 6G. middle	Band power	n=7	Holm-Šidák	Delta	0.3745	ns	t=0.9225
				Theta	0.5943	ns	t=0.5506
Fig. 6G. right	Band power	n=7	Holm-Šidák	Delta	0.1671	ns	t=1.531
				Theta	0.8701	ns	t=0.1672
Fig. 6H. left	Band power	n=6	Holm-Šidák	Delta	0.5244	ns	t=0.6529
				Theta	0.2624	ns	t=1.168
Fig. 6H. middle	Band power	n=6	Holm-Šidák	Delta	0.05167	ns	t=2.127
				Theta	0.01365	*	t=2.819
Fig. 6H. right	Band power	n=6	Holm-Šidák	Delta	0.3086	ns	t=1.057
				Theta	0.04454	*	t=2.207

SUPPLEMENTARY FIGURES

fig. S1

Panel	Data	Group size	Statistic method	Comparison	*P* value	Notation	F/q statistic
fig. S1A	Wake amount/h	n=6 each group	Two-way RM ANOVA, Post-hoc Šidák	Main effect of group	0.0693	ns	$F_{(1, 10)}$=8.229
fig. S1B	Wake bout count/h	n=5 each group	Two-way RM ANOVA, Post-hoc Šidák	Main effect of group	<0.0001	†	$F_{(1, 10)}$=42.89
fig. S1C	Mean wake bout length	n=6 each group	Two-way RM ANOVA, Post-hoc Šidák	Main effect of group	0.0008	****	$F_{(1, 10)}$=22.60
fig. S1D	Total wake bout length	n=6 each group	Holm-Šidák	48 hour	0.01754	*	t=2.840
				Light	0.7952	ns	t=0.2666
				Dark	0.004842	***	t=3.601
fig. S1E	Total wake bout count	n=6 each group	Holm-Šidák	48 hour	<0.0001	†	t=8.872
				Light	0.004348	***	t=3.085
				Dark	<0.0001	†	t=5.787
fig. S1F	Mean wake bout length	n=6 each group	Holm-Šidák	48 hour	0.0009415	****	t=4.626
				Light	0.004970	***	t=3.585
				Dark	0.003951	***	t=3.724
fig. S1G	NREM amount/h	n=6 each group	Two-way RM ANOVA, Post-hoc Šidák	Main effect of group	0.0137	*	$F_{(1, 10)}$=8.902
fig. S1H	NREM bout count/h	n=6 each group	Two-way RM ANOVA, Post-hoc Šidák	Main effect of group	<0.0001	†	$F_{(1, 10)}$=45.83
fig. S1I	Mean NREM bout length	n=6 each group	Two-way RM ANOVA, not applicable (N/A)	Main effect of group	N/A	N/A	N/A
fig. S1J	Total NREM bout length	n=6 each group	Holm-Šidák	48 hour	0.01259	*	t=3.034
				Light	0.7923	ns	t=0.2704
				Dark	0.002725	***	t=3.951
fig. S1K	Total NREM bout count	n=6 each group	Holm-Šidák	48 hour	<0.0001	†	t=6.769
				Light	0.0009419	****	t=4.626
				Dark	<0.0001	†	t=7.136
fig. S1L	Mean NREM bout length	n=6 each group	Holm-Šidák	48 hour	<0.0001	†	t=6.892
				Light	0.0009381	****	t=4.629
				Dark	<0.0001	†	t=6.531
fig. S1M	REM amount/h	n=6 each group	Two-way RM ANOVA, Post-hoc Šidák	Main effect of group	0.5170	ns	$F_{(1, 10)}$ =0.4512
fig. S1N	REM bout count/h	n=6 each group	Two-way RM ANOVA, Post-hoc Šidák	Main effect of group	0.3085	ns	$F_{(1, 10)}$=1.151
fig. S1O	Mean REM bout length	n=6 each group	Two-way RM ANOVA, not applicable (N/A)	Main effect of group	N/A	N/A	N/A
fig. S1P	Total REM bout length	n=6 each group	Holm-Šidák	48 hour	0.5120	ns	t=0.6798
				Light	0.9875	ns	t=0.01607
				Dark	0.4113	ns	t=0.8573
fig. S1Q	Total REM bout count	n=6 each group	Holm-Šidák	48 hour	0.3085	ns	t=1.073
				Light	>0.9999	ns	t=0
				Dark	0.3219	ns	t=1.042

fig. S1R	Mean REM bout length	n=6 each group	Holm-Šidák	48 hour	0.9750	ns	t=0.03210
				Light	0.9588	ns	t=0.05293
				Dark	0.8881	ns	t=0.1443

fig. S2

Panel	Data	Group size	Statistic method	Comparison	*P* value	Notation	F/t statistic
fig. S2E	Hcrt neuron count	Young: n=6 Aged: n=6	Two-way ANOVA	Anterior-posterior location (APL)	<0.0001	†	$F_{(24, 250)}$= 311.4
				Age	<0.0001	†	$F_{(1, 250)}$= 950.0
				Interaction	<0.0001	†	$F_{(24, 250)}$= 13.74
			Šidák's multiple comparisons	APL -1.000	<0.0001	†	t=6.359
				APL -1.035	0.8011	ns	t=0.2586
				APL -1.070	0.0006308	****	t=4.892
				APL -1.105	<0.0001	†	t=6.248
				APL -1.140	<0.0001	†	t=7.628
				APL -1.175	<0.0001	†	t=6.814
				APL -1.210	<0.0001	†	t=8.256
				APL -1.245	<0.0001	†	t=9.862
				APL -1.280	<0.0001	†	t=8.695
				APL -1.315	<0.0001	†	t=9.085
				APL -1.350	<0.0001	†	t=7.579
				APL -1.385	0.009288	**	t=3.213
				APL -1.420	<0.0001	†	t=9.663
				APL -1.455	<0.0001	†	t=9.900
				APL -1.490	<0.0001	†	t=11.84
				APL -1.525	<0.0001	†	t=10.15
				APL -1.560	<0.0001	†	t=7.541
				APL -1.595	0.0007528	****	t=4.774
				APL -1.630	<0.0001	†	t=9.516
				APL -1.665	<0.0001	†	t=6.355
				APL -1.700	0.01814	*	t=2.821
				APL -1.735	0.002556	***	t=3.991
				APL -1.770	0.0007529	****	t=4.774
				APL -1.805	0.02011	*	t=2.760
				APL -1.840	0.02628	*	t=2.605
fig. S2E. Inset	Hcrt neuron count	Young: n=6 Aged: n=6	Unpaired *t*-test	Young vs. Aged	<0.0001	†	t=20.09

fig. S3

Panel	Data	Group size	Statistic method	Comparison	*P* value	Notation	F/t statistic
fig. S3B	ChR2-eYFP+ cell count	Young: n = 8 vs. Aged: n = 8	Mann-Whitney *U* test	Young vs. Aged	0.0499	*	N/A
fig. S3C	Percentage of ChR2-eYFP neurons positive for Hcrt1	Young: n = 8 vs. Aged: n = 8	Mann-Whitney *U* test	Young vs. Aged	0.7209	ns	N/A

fig. S4

Panel	Data	Group size	Statistic method	Comparison	*P* value	Notation	F/t statistic
fig. S4C	PSC failure percentage	Young: n=15 Aged: n=18	Two-way ANOVA	Stimulation Frequency (Hz)	<0.0001	†	$F_{(4, 153)}$=14.87
				Age	0.0059	**	$F_{(1, 153)}$=7.813
				Interaction	0.8490	ns	$F_{(4, 153)}$=0.3424
			Post-hoc Šidák's multiple comparisons	1 Hz	0.9944	ns	t=0.4609
				5 Hz	0.8545	ns	t=0.9979
				10 Hz	0.7500	ns	t=1.174
				15 Hz	0.2477	ns	t=1.931
				20 Hz	0.3973	ns	t=1.673

fig. S5

Panel	Data	Group size	Statistic method	Comparison	P value	Notation
fig. S5D	Hcrt	Young: n=225 vs. Aged: n=129	Wilcoxon rank-sum test	Young vs. Aged	2.98e-11	†
	Gm42418	Young: n=225 vs. Aged: n=129	Wilcoxon rank-sum test	Young vs. Aged	3.73e-12	†
	6330403Rik	Young: n=225 vs. Aged: n=129	Wilcoxon rank-sum test	Young vs. Aged	1.02e-4	†
	Peg3	Young: n=225 vs. Aged: n=129	Wilcoxon rank-sum test	Young vs. Aged	4.68e-5	†
	Unc5c	Young: n=225 vs. Aged: n=129	Wilcoxon rank-sum test	Young vs. Aged	0.0422	*

fig. S6

Panel	Group size	Statistic method	Comparison	Data	*P* value
fig. S6D	Young: n=170 Aged: n =165	Wilcoxon rank-sum test	Young vs. Aged	Hcrt	3.87E-49
				6330403K07Rik	6.39E-20
				Zfp804b	1.05E-17
				Ndn	1.26E-17
				Nnat	4.08E-17
				Ubb	8.27E-14
				Cdh20	3.97E-11
				Oxr1	4.51E-11
				Itm2b	6.47E-11
				Pcsk1n	1.18E-10
				Fth1	1.45E-10
				Ptpn5	1.50E-10
				Ppia	1.66E-10
				Fstl5	2.84E-10
				Grid2	3.75E-10
				Nenf	4.60E-10
				Erc2	5.13E-10
				Gm42418	7.57E-10
				C030034L19Rik	9.35E-10
				Dlgap1	1.20E-09
				Gnas	1.27E-09
				Tox	1.31E-09
				Wipf3	6.52E-09
				Gucy1a2	7.77E-09
				Stmn3	8.34E-09
				Arhgap26	1.72E-08
				Cst3	1.87E-08
				RP23-407N2.2	2.41E-08
				Tmem114	2.91E-08
				Mical2	3.67E-08
				Atp1a3	3.72E-08
				Map3k4	5.08E-08
				Gm9843	9.37E-08
				Nbea	9.39E-08
				Magi3	1.02E-07
				Ank3	1.68E-07
				Dok5	1.92E-07
				Sema6a	2.15E-07
				Ghr	2.42E-07
				Ralgapa2	2.50E-07
				Bsg	2.55E-07
				Htr2c	3.40E-07
				Dab1	3.52E-07
				Cacna1a	4.07E-07
				C1ql3	4.57E-07
				Pcp4	6.50E-07
				Smyd4	6.92E-07

				Trpc7	1.00E-06
				Cfap77	1.18E-06
				PISD	1.25E-06
				Slc25a48	1.32E-06
				Cox8a	1.35E-06
				Uchl1	1.57E-06
				Rasgrf2	1.61E-06
				Epha5	1.71E-06
				9530052E02Rik	1.76E-06
				Tanc2	1.77E-06
				Dnah9	1.78E-06
				Arhgap39	1.79E-06
				2900026A02Rik	2.07E-06
				Vwc2l	2.65E-06
				Mkl2	2.89E-06
				Lrp1b	3.02E-06
				Adck4	3.02E-06

fig. S7

Panel	Data	Group size	Statistic method	Comparison	*P* value	Notation	F/t statistic
fig. S7A Week1 top panel 1	Wake amount/2h	n=5 each group	Two-way RM ANOVA, Post-hoc Šidák	Main effect of group	0.6959	ns	$F_{(1, 8)}$= 0.1642
fig. S7A Week1 top panel 2	Wake bout count/2h	n=5 each group	Two-way RM ANOVA, Post-hoc Šidák	Main effect of group	0.9533	ns	$F_{(1, 8)}$= 0.003655
fig. S7A Week1 top panel 3	Mean wake bout length	n=5 each group	Two-way RM ANOVA, Post-hoc Šidák	Main effect of group	0.8158	ns	$F_{(1, 8)}$= 0.05769
fig. S7A Week1 top panel 4	Mean wake bout length	n=5 each group	Holm-Šidák	48 hour	0.8152	ns	t=0.2415
				Light	0.2665	ns	t=1.194
				Dark	0.5826	ns	t=0.5726
fig. S7A Week1 middle panel 1	NREM amount/2h	n=5 each group	Two-way RM ANOVA, Post-hoc Šidák	Main effect of group	0.8085	ns	$F_{(1, 8)}$= 0.06274
fig. S7A Week1 middle panel 2	NREM bout count/2h	n=5 each group	Two-way RM ANOVA, Post-hoc Šidák	Main effect of group	0.9888	ns	$F_{(1, 8)}$= 0.0002100
fig. S7A Week1 middle panel 3	Mean NREM bout length	n=5 each group	Two-way RM ANOVA, Post-hoc Šidák	Main effect of group	0.5359	ns	$F_{(1, 8)}$= 0.4182
fig. S7A Week1 middle panel 4	Mean NREM bout length	n=5 each group	Holm-Šidák	48 hour	0.6624	ns	t=0.4532
				Light	0.8018	ns	t=0.2594
				Dark	0.7870	ns	t=0.2794
fig. S7A Week1 bottom panel 1	REM amount/2h	n=5 each group	Two-way RM ANOVA, Post-hoc Šidák	Main effect of group	0.5871	ns	$F_{(1, 8)}$= 0.3200
fig. S7A Week1 bottom panel 2	REM bout count/2h	n=5 each group	Two-way RM ANOVA, Post-hoc Šidák	Main effect of group	0.5325	ns	$F_{(1, 8)}$= 0.4255
fig. S7A Week1 bottom panel 3	Mean REM bout length	n=5 each group	Two-way RM ANOVA, not applicable (N/A)	Main effect of group	N/A	N/A	N/A
fig. S7A Week1 bottom panel 4	Mean REM bout length	n=5 each group	Holm-Šidák	48 hour	0.8666	ns	t=0.1734
				Light	0.8800	ns	t=0.1558
				Dark	0.5272	ns	t=0.6609
fig. S7A Week12 top panel 1	Wake amount/2h	n=5 each group	Two-way RM ANOVA, Post-hoc Šidák	Main effect of group	0.6404	ns	$F_{(1, 8)}$= 0.2357
fig. S7A Week12 top panel 2	Wake bout count/2h	n=5 each group	Two-way RM ANOVA, Post-hoc Šidák	Main effect of group	0.0223	*	$F_{(1, 8)}$=7.986
fig. S7A Week12 top panel 3	Mean wake bout length	n=5 each group	Two-way RM ANOVA, Post-hoc Šidák	Main effect of group	0.0538	ns	$F_{(1, 8)}$= 5.102
fig. S7A Week12 top panel 4	Mean wake bout length	n=5 each group	Holm-Šidák	48 hour	0.08493	ns	t=1.966
				Light	0.2016	ns	t=1.391
				Dark	0.06666	ns	t=2.122

fig. S7A Week12 middle panel 1	NREM amount/2h	n=5 each group	Two-way RM ANOVA, Post-hoc Šidák	Main effect of group	0.9113	ns	$F_{(1, 8)}$= 0.01323
fig. S7A Week12 middle panel 2	NREM bout count/2h	n=5 each group	Two-way RM ANOVA, Post-hoc Šidák	Main effect of group	0.0243	*	$F_{(1, 8)}$=7.672
fig. S7A Week12 middle panel 3	Mean NREM bout length	n=5 each group	Two-way RM ANOVA, Post-hoc Šidák	Main effect of group	0.0126	*	$F_{(1, 8)}$=10.24
fig. S7A Week12 middle panel 4	Mean NREM bout length	n=5 each group	Holm-Šidák	48 hour	0.009404	**	t=3.397
				Light	0.005076	**	t=3.822
				Dark	0.035939	*	t=2.518
fig. S7A Week12 bottom panel 1	REM amount/2h	n=5 each group	Two-way RM ANOVA, Post-hoc Šidák	Main effect of group	0.0121	*	$F_{(1, 8)}$=10.43
fig. S7A Week12 bottom panel 2	REM bout count/2h	n=5 each group	Two-way RM ANOVA, Post-hoc Šidák	Main effect of group	0.0241	*	$F_{(1, 8)}$=7.709
fig. S7A Week12 bottom panel 3	Mean REM bout length	n=5 each group	Two-way RM ANOVA, Post-hoc Šidák	Main effect of group	0.0706	ns	$F_{(1, 8)}$=4.345
fig. S7A Week12 bottom panel 4	Mean REM bout length	n=5 each group	Holm-Šidák	48 hour	0.1164	ns	t=1.760
				Light	0.1115	ns	t=1.788
				Dark	0.2575	ns	t=1.219
fig. S7C	RMP	sgControl: 33 vs. sgKcnq2/3: 22	Mann-Whitney *U* test	sgControl vs. sgKcnq2/3	0.0142	*	N/A
fig. S7F top panel 1	RMP	n=15 each group	Mann-Whitney *U* test	sgControl vs. sgKcnq2/3	0.0367	*	N/A
fig. S7F top panel 2	Firing threshold	n=15 each group	Mann-Whitney *U* test	sgControl vs. sgKcnq2/3	0.0169	*	N/A
fig. S7F top panel 3	Difference between RMP and threshold	n=15 each group	Mann-Whitney *U* test	sgControl vs. sgKcnq2/3	0.9674	ns	N/A
fig. S7F top panel 4	Amplitude of AP	n=15 each group	Mann-Whitney *U* test	sgControl vs. sgKcnq2/3	0.3892	ns	N/A
fig. S7F bottom panel 1	Risetime of AP	n=15 each group	Mann-Whitney *U* test	sgControl vs. sgKcnq2/3	0.1485	ns	N/A
fig. S7F bottom panel 2	Half duration of AP	n=15 each group	Mann-Whitney *U* test	sgControl vs. sgKcnq2/3	0.3669	ns	N/A
fig. S7F bottom panel 3	Max. rising slope	n=15 each group	Mann-Whitney *U* test	sgControl vs. sgKcnq2/3	0.0425	*	N/A
fig. S7F bottom panel 4	Max. decaying slope	n=15 each group	Mann-Whitney *U* test	sgControl vs. sgKcnq2/3	0.2895	ns	N/A

fig. S8

Panel	Data	Group size	Statistic method	Comparison	*P* value	Notation	t statistic
fig. S8B	Exploration of identical objects	n=9	Unpaired *t*-test with Welch's correction	IO1 vs. IO2	0.6496	ns	t=0.4630
fig. S8C	Exploration of familiar object	n=9	Unpaired *t*-test with Welch's correction	Vehicle vs. flupirtine	0.04402	*	t=2.186
fig. S8C	Exploration of novel object	n=9	Unpaired *t*-test with Welch's correction	Vehicle vs. flupirtine	0.04402	*	t=2.186

fig. S9

Panel	Data	Group size	Statistic method	Comparison	*P* value	Notation	F/q statistic
fig. S9C row 1 No.1	Wake amount/h	n=6 each group	Two-way RM ANOVA, Post-hoc Šidák	Main effect of group	0.5683	ns	$F_{(1, 10)}$= 0.3481
fig. S9C row 1 No.2	Wake bout count/h	n=6 each group	Two-way RM ANOVA, Post-hoc Šidák	Main effect of group	0.3136	ns	$F_{(1, 10)}$= 1.126

fig. S9C row 1 No.3	Mean wake bout length	n=6 each group	Two-way RM ANOVA, Post-hoc Šidák	Main effect of group	0.0242	*	$F_{(1, 10)}$= 7.304
fig. S9C row 1 No.4	Total wake bout length	n=6 each group	Holm-Šidák	48 hour	0.8892	ns	t=0.1429
				Light	0.4001	ns	t=0.8788
				Dark	0.4905	ns	t=0.7158
fig. S9C row 1 No.5	Total wake bout count	n=6 each group	Holm-Šidák	48 hour	0.1534	ns	t=1.465
				Light	0.2926	ns	t=1.071
				Dark	0.6966	ns	t=0.3936
fig. S9C row 1 No.6	Mean wake bout length	n=6 each group	Holm-Šidák	48 hour	0.4665	ns	t=0.7570
				Light	0.08281	ns	t=1.927
				Dark	0.9675	ns	t=0.04182
fig. S9C row 2 No.1	NREM amount/h	n=6 each group	Two-way RM ANOVA, Post-hoc Šidák	Main effect of group	0.7640	ns	$F_{(1, 10)}$= 0.09520
fig. S9C row 2 No.2	NREM bout count/h	n=6 each group	Two-way RM ANOVA, Post-hoc Šidák	Main effect of group	0.2682	ns	$F_{(1, 10)}$= 1.375
fig. S9C row 2 No.3	Mean NREM bout length	n=6 each group	Two-way RM ANOVA, Post-hoc Šidák	Main effect of group	0.0544	ns	$F_{(1, 10)}$= 4.743
fig. S9C row 2 No.4	Total NREM bout length	n=6 each group	Holm-Šidák	48 hour	0.7589	ns	t=0.3155
				Light	0.3089	ns	t=1.072
				Dark	0.3439	ns	t=0.9936
fig. S9C row 2 No.5	Total NREM bout count	n=6 each group	Holm-Šidák	48 hour	0.2682	ns	t=1.172
				Light	0.1250	ns	t=1.674
				Dark	0.6183	ns	t=0.5141
fig. S9C row 2 No.6	Mean NREM bout length	n=6 each group	Holm-Šidák	48 hour	0.2572	ns	t=1.202
				Light	0.3534	ns	t=0.9732
				Dark	0.1443	ns	t=1.584
fig. S9C row 3 No.1	REM amount/h	n=6 each group	Two-way RM ANOVA, Post-hoc Šidák	Main effect of group	0.7683	ns	$F_{(1, 10)}$ = 0.09161
fig. S9C row 3 No.2	REM bout count/h	n=6 each group	Two-way RM ANOVA, Post-hoc Šidák	Main effect of group	0.2481	ns	$F_{(1, 10)}$= 1.505
fig. S9C row 3 No.3	Mean REM bout length	n=6 each group	Two-way RM ANOVA, Post-hoc Šidák	Main effect of group	0.0170	*	$F_{(1, 10)}$ = 8.170
fig. S9C row 3 No.4	Total REM bout length	n=6 each group	Holm-Šidák	48 hour	0.7699	ns	t=0.3005
				Light	0.9216	ns	t=0.1009
				Dark	0.4326	ns	t=0.8176
fig. S9C row 3 No.5	Total REM bout count	n=6 each group	Holm-Šidák	48 hour	0.2480	ns	t=1.227
				Light	0.3382	ns	t=1.006
				Dark	0.5212	ns	t=0.6648
fig. S9C row 3 No.6	Mean REM bout length	n=6 each group	Holm-Šidák	48 hour	0.01386	*	t=2.978
				Light	0.02968	*	t=2.534
				Dark	0.04045	*	t=2.353
fig. S9C row 4 No.1	Cataplexy-like amount/h	n=6 each group	Two-way RM ANOVA, Post-hoc Šidák	Main effect of group	0.1464	ns	$F_{(1, 10)}$= 2.480
fig. S9C row 4 No.2	Cataplexy-like bout count/h	n=6 each group	Two-way RM ANOVA, Post-hoc Šidák	Main effect of group	0.1114	ns	$F_{(1, 10)}$= 3.049
fig. S9C row 4 No.3	Mean cataplexy-like bout length	n=6 each group	Two-way RM ANOVA, Not applicable (N/A)	Main effect of group	N/A	N/A	N/A
fig. S9C row 4 No.4	Total cataplexy-like bout length	n=6 each group	Holm-Šidák	24 hour	0.1464	ns	t=1.575
				Light	N/A	N/A	N/A
				Dark	0.1464	ns	t=1.575
fig. S9C row 4 No.5	Total cataplexy-like bout count	n=6 each group	Holm-Šidák	24 hour	0.1114	ns	t=1.746
				Light	N/A	N/A	N/A
				Dark	0.1114	ns	t=1.746
fig. S9C row 4 No.6	Mean cataplexy-like bout length	n=6 each group	Holm-Šidák	24 hour	N/A	N/A	N/A
				Light	N/A	N/A	N/A
				Dark	N/A	N/A	N/A

fig. S9G panel 1	RMP	Control: n=17 vs. ataxin3$^+$: n=21	Mann-Whitney *U* test	Control vs. ataxin3$^+$	0.0179	*	N/A
fig. S9G panel 2	Firing threshold	Control: n=17 vs. ataxin3$^+$: n=21	Mann-Whitney *U* test	Control vs. ataxin3$^+$	0.1673	ns	N/A
fig. S9G panel 3	Difference between RMP and threshold	Control: n=17 vs. ataxin3$^+$: n=21	Mann-Whitney *U* test	Control vs. ataxin3$^+$	0.0161	*	N/A
fig. S9G panel 4	Amplitude of AP	Control: n=17 vs. ataxin3$^+$: n=21	Mann-Whitney *U* test	Control vs. ataxin3$^+$	0.6217	ns	N/A
fig. S9G panel 5	Risetime of AP	Control: n=17 vs. ataxin3$^+$: n=21	Mann-Whitney *U* test	Control vs. ataxin3$^+$	0.7717	ns	N/A
fig. S9G panel 6	Half duration of AP	Control: n=17 vs. ataxin3$^+$: n=21	Mann-Whitney *U* test	Control vs. ataxin3$^+$	0.3990	ns	N/A
fig. S9G panel 7	Max. rising slope	Control: n=17 vs. ataxin3$^+$: n=21	Mann-Whitney *U* test	Control vs. ataxin3$^+$	0.9307	ns	N/A
fig. S9G panel 8	Max. decaying slope	Control: n=17 vs. ataxin3$^+$: n=21	Mann-Whitney *U* test	Control vs. ataxin3$^+$	0.2943	ns	N/A

fig. S10

Panel	**Data**	**Group size**	**Statistic method**	**Comparison**	***P* value**	**Notation**	**F/q statistic**
fig. S10A row 1 No.1	Wake amount/h	n=6 each group	Two-way RM ANOVA, Post-hoc Šidák	Main effect of group	0.0875	ns	$F_{(1, 10)}$= 3.587
Fig. S10A row 1 No.2	Wake bout count/h	n=6 each group	Two-way RM ANOVA, Post-hoc Šidák	Main effect of group	0.0006	****	$F_{(1, 10)}$= 24.30
fig. S10A row 1 No.3	Mean wake bout length	n=6 each group	Two-way RM ANOVA, Post-hoc Šidák	Main effect of group	0.0021	***	$F_{(1, 10)}$= 16.95
fig. S10A row 1 No.4	Total wake bout length	n=6 each group	Holm-Šidák	24 hour	0.08632	ns	t=1.902
				Light	0.1123	ns	t=1.741
				Dark	0.004660	***	t=3.624
fig. S10A row 1 No.5	Total wake bout count	n=6 each group	Holm-Šidák	24 hour	<0.0001	†	t=6.691
				Light	0.1597	ns	t=1.442
				Dark	<0.0001	†	t=5.249
fig. S10A row 1 No.6	Mean wake bout length	n=6 each group	Holm-Šidák	24 hour	0.005495	**	t=3.525
				Light	0.6216	ns	t=0.5092
				Dark	0.008482	**	t=4.695
fig. S10A row 2 No.1	NREM amount/h	n=6 each group	Two-way RM ANOVA, Post-hoc Šidák	Main effect of group	0.2200	ns	$F_{(1, 10)}$= 1.712
fig. S10A row 2 No.2	NREM bout count/h	n=6 each group	Two-way RM ANOVA, Post-hoc Šidák	Main effect of group	0.0013	***	$F_{(1, 10)}$= 19.59
fig. S10A row 2 No.3	Mean NREM bout length	n=6 each group	Two-way RM ANOVA, Post-hoc Šidák	Main effect of group	0.0021	***	$F_{(1, 10)}$= 16.95
fig. S10A row 2 No.4	Total NREM bout length	n=6 each group	Holm-Šidák	24 hour	0.2218	ns	t=1.303
				Light	0.1263	ns	t=1.668
				Dark	0.01681	*	t=2.865
fig. S10A row 2 No.5	Total NREM bout count	n=6 each group	Holm-Šidák	24 hour	0.001282	***	t=4.426
				Light	0.08415	ns	t=1.918
				Dark	0.0001270	†	t=6.030
fig. S10A row 2 No.6	Mean NREM bout length	n=6 each group	Holm-Šidák	24 hour	0.0002890	†	t=5.430
				Light	0.006460	**	t=3.428
				Dark	<0.0001	†	t=7.276
fig. S10A row 3 No.1	REM amount/h	n=6 each group	Two-way RM ANOVA, Post-hoc Šidák	Main effect of group	0.2523	ns	$F_{(1, 10)}$= 1.476
fig. S10A row 3 No.2	REM bout count/h	n=6 each group	Two-way RM ANOVA, Post-hoc Šidák	Main effect of group	0.5637	ns	$F_{(1, 10)}$= 0.3566
fig. S10A row 3 No.3	Mean REM bout length	n=6 each group	Two-way RM ANOVA, not applicable (N/A)	Main effect of group	N/A	N/A	N/A
			Holm-Šidák	24 hour	0.2539	ns	t=1.211

fig. S10A row 3 No.4	Total REM bout length	n=6 each group		Light	0.2776	ns	t=1.148
				Dark	0.01028	*	t=3.153
fig. S10A row 3 No.5	Total REM bout count	n=6 each group	Holm-Šidák	24 hour	0.5637	ns	t=0.5972
				Light	0.3619	ns	t=0.9555
				Dark	0.04419	*	t=2.301
fig. S10A row 3 No.6	Mean REM bout length	n=6 each group	Holm-Šidák	24 hour	0.4048	ns	t=0.8698
				Light	0.9974	ns	t=0.003295
				Dark	0.3372	ns	t=0.1673
fig. S10A row 4 No.1	Cataplexy-like amount/h	n=6 each group	Two-way RM ANOVA, Post-hoc Šidák	Main effect of group	0.0026	***	$F_{(1, 10)}$= 15.85
fig. S10A row 4 No.2	Cataplexy-like bout count/h	n=6 each group	Two-way RM ANOVA, Post-hoc Šidák	Main effect of group	0.0026	***	$F_{(1, 10)}$= 15.85
fig. S10A row 4 No.3	Mean cataplexy-like bout length	n=6 each group	Two-way RM ANOVA, not applicable (N/A)	Main effect of group	N/A	N/A	N/A
fig. S10A row 4 No.4	Total cataplexy-like bout length	n=6 each group	Holm-Šidák	24 hour	0.002598	***	t=3.981
				Light	0.017725	*	t=2.834
				Dark	0.002642	***	t=3.970
fig. S10A row 4 No.5	Total cataplexy-like bout count	n=6 each group	Holm-Šidák	24 hour	0.002595	***	t=3.981
				Light	0.07792	ns	t=1.964
				Dark	0.001154	***	t=4.494
fig. S10A row 4 No.6	Mean cataplexy-like bout length	n=6 each group	Holm-Šidák, not applicable (N/A)	24 hour	N/A	N/A	N/A
				Light	N/A	N/A	N/A
				Dark	N/A	N/A	N/A

fig. S11

Panel	Data	Group size	Statistic method	Comparison	***P* value**	Notation	F/t statistic
fig. S11A	Wake (%/h)	n=9	Two-way mixed effects model, Post-hoc Šidák	Time	<0.0001	†	$F_{(23, 368)}$=15.92
				Treatment	0.0411	*	$F_{(1, 16)}$=4.937
				Interaction	0.2936	ns	$F_{(23, 368)}$=1.145
fig. S11B	Wake bout count/h	n=9	Two-way mixed effects model, Post-hoc Šidák	Time	0.0002	†	$F_{(23, 368)}$=3.916
				Treatment	0.5886	ns	$F_{(1, 16)}$=0.3046
				Interaction	0.5552	ns	$F_{(23, 368)}$=0.9320
fig. S11C	Mean wake bout length	n=9	Two-way mixed effects model, Post-hoc Šidák	Time	0.0512	ns	$F_{(23, 368)}$=2.435
				Treatment	0.4193	ns	$F_{(1, 16)}$=0.6871
				Interaction	0.4699	ns	$F_{(23, 368)}$=0.9957
fig. S11D	Total wake bout length	n=9	Holm-Šidák	ZT 0-6	0.0418	*	t=2.213
				ZT 6-12	0.7239	ns	t=0.3595
				ZT 12-18	0.4814	ns	t=0.7209
				ZT 18-24	0.3274	ns	t=1.010
fig. S11E	Total wake bout count	n=9	Holm-Šidák	ZT 0-6	0.4040	ns	t=0.8400
				ZT 6-12	0.9432	ns	t=0.07149
				ZT 12-18	0.3942	ns	t=0.8579
				ZT 18-24	0.3122	ns	t=1.019
fig. S11F	Mean wake bout length	n=9	Holm-Šidák	ZT 0-6	0.04126	*	t=2.219
				ZT 6-12	0.9993	ns	t=0.0008554
				ZT 12-18	0.2896	ns	t=1.095
				ZT 18-24	0.2148	ns	t=1.292
fig. S11G	NREM (%/h)	n=9	Two-way mixed effects model, Post-hoc Šidák	Time	<0.0001	†	$F_{(23, 368)}$=16.68
				Treatment	0.0910	ns	$F_{(1, 16)}$=3.235
				Interaction	3.3135	ns	$F_{(23, 368)}$=1.126
fig. S11H	NREM bout count/h	n=9	Two-way mixed effects model, Post-hoc Šidák	Time	<0.0001	†	$F_{(23, 368)}$=4.706
				Treatment	0.7341	ns	$F_{(1, 16)}$=0.1195
				Interaction	0.7071	ns	$F_{(23, 368)}$=0.8194
fig. S11I	Mean NREM bout length	n=9	Two-way mixed effects model, Post-hoc Šidák	Time	<0.0001	†	$F_{(23, 363)}$=16.14
				Treatment	0.0619	ns	$F_{(1, 16)}$=4.030
				Interaction	0.0003	†	$F_{(23, 363)}$=2.431
fig. S11J		n=9	Holm-Šidák	ZT 0-6	0.01823	*	t=2.629

	Total NREM bout length			ZT 6-12	0.7822	ns	t=0.2811
				ZT 12-18	0.4673	ns	t=0.7445
				ZT 18-24	0.3453	ns	t=0.9724
fig. S11K	Total NREM bout count	n=9	Holm-Šidák	ZT 0-6	0.2736	ns	t=1.134
				ZT 6-12	0.9222	ns	t=0.09915
				ZT 12-18	0.2514	ns	t=1.190
				ZT 18-24	0.3508	ns	t=0.9611
fig. S11L	Mean NREM bout length	n=9	Holm-Šidák	ZT 0-6	0.01018	*	t=2.912
				ZT 6-12	0.6639	ns	t=0.4427
				ZT 12-18	0.6235	ns	t=0.5005
				ZT 18-24	0.7968	ns	t=0.2618
fig. S11M	REM (%/h)	n=9	Two-way mixed effects model, Post-hoc Šidák	Time	<0.0001	†	$F_{(23, 368)}$=9.096
				Treatment	0.9503	ns	$F_{(1, 16)}$ =0.004001
				Interaction	0.4001	ns	$F_{(23, 368)}$=1.051
fig. S11N	REM bout count/h	n=9	Two-way mixed effects model, Post-hoc Šidák	Time	<0.0001	†	$F_{(23, 368)}$=10.62
				Treatment	0.9723	ns	$F_{(1, 16)}$ =0.001241
				Interaction	0.0601	ns	$F_{(23, 368)}$=1.521
fig. S11O	Mean REM bout length	n=9	Two-way mixed effects model, Post-hoc Šidák	Time	0.0550	ns	$F_{(23, 297)}$=2.238
				Treatment	0.4222	ns	$F_{(1, 16)}$=0.6785
				Interaction	0.8513	ns	$F_{(23, 297)}$=0.6941
fig. S11P	Total REM bout length	n=9	Holm-Šidák	ZT 0-6	0.9005	ns	t=0.1270
				ZT 6-12	0.8062	ns	t=0.2494
				ZT 12-18	0.6815	ns	t=0.4181
				ZT 18-24	0.3431	ns	t=0.9769
fig. S11Q	Total REM bout count	n=9	Holm-Šidák	ZT 0-6	0.9231	ns	t=0.09806
				ZT 6-12	>0.9999	ns	t=0
				ZT 12-18	0.3876	ns	t=0.8883
				ZT 18-24	0.3433	ns	t=0.9766
fig. S11R	Mean REM bout length	n=9	Holm-Šidák	ZT 0-6	0.3786	ns	t=0.9055
				ZT 6-12	0.1846	ns	t=1.386
				ZT 12-18	0.09061	ns	t=1.801
				ZT 18-24	0.9345	ns	t=0.08353

fig. S12

Panel	Data	Group size	Statistic method	Comparison	*P* value	Notation	F/t statistic
fig. S12E	LC NA neuron count	Young: n=6 vs. Aged: n =6	Two-way ANOVA	Anterior-posterior location (APL)	<0.0001	†	$F_{(31, 320)}$=521.3
				Age	<0.0001	†	$F_{(1, 320)}$=162.2
				Interaction	<0.0001	†	$F_{(31, 320)}$=10.62
			Šidák's multiple comparisons	APL -4.945	0.9451	ns	t=0.07068
				APL -4.980	0.5883	ns	t=0.5592
				APL -5.015	0.02556	*	t=2.621
				APL -5.050	0.4425	ns	t=0.7996
				APL -5.085	0.4754	ns	t=0.7415
				APL -5.120	0.5415	ns	t=0.4800
				APL -5.155	0.8287	ns	t=0.2221
				APL -5.190	0.8366	ns	t=0.2118
				APL -5.225	0.000394	†	t=5.213
				APL -5.260	0.000287	†	t=5.435
				APL -5.295	0.000129	†	t=6.018
				APL -5.330	<0.0001	†	t=11.09
				APL -5.365	<0.0001	†	t=8.287
				APL -5.400	<0.0001	†	t=9.613
				APL -5.435	<0.0001	†	t=6.933
				APL -5.470	0.1133	ns	t=1.736
				APL -5.505	0.1539	ns	t=1.543
				APL -5.540	0.9929	ns	t=0.009130

				APL -5.575	0.7936	ns	t=0.2687
				APL -5.610	0.000790	****	t=4.741
				APL -5.645	0.04279	*	t=2.320
				APL -5.680	0.06848	ns	t=2.041
				APL -5.715	0.8040	ns	t=0.2549
				APL -5.750	0.9570	ns	t=0.05530
				APL -5.785	0.5344	ns	t=0.6434
				APL -5.820	0.01831	*	t=2.815
				APL -5.855	0.04419	*	t=2.301
				APL -5.890	0.4078	ns	t=0.8642
				APL -5.925	0.6317	ns	t=0.4944
				APL -5.960	0.0064	**	t=3.432
				APL -5.995	0.6867	ns	t=0.4152
				APL -6.030	0.9106	ns	t=0.1152
fig. S12E. Inset	LC NA neuron count	Young: n=6 vs. Aged: n=6	Unpaired *t*-test	Young vs. Aged	<0.0001	†	t=6.654

fig. S13

Panel	Data	Group size	Statistic method	Comparison condition	*P* value	Notation	F/t statistic
fig. S13B	Latency for NREM-to-wake transition across stimulation parameters: Young vs. Aged	n=8 mice each group	Mann-Whitney *U* test	1 mW, 1 Hz	0.04988	*	N/A
				1 mW, 5 Hz	0.00078	****	N/A
				1 mW, 10 Hz	0.00777	**	N/A
				1 mW, 15 Hz	0.00218	***	N/A
				1 mW, 20 Hz	0.18197	ns	N/A
				5 mW, 1 Hz	0.04988	*	N/A
				5 mW, 5 Hz	0.00078	****	N/A
				5 mW, 10 Hz	0.00124	***	N/A
				5 mW, 15 Hz	0.01585	*	N/A
				5 mW, 20 Hz	0.04600	*	N/A
				10 mW, 1 Hz	0.02580	*	N/A
				10 mW, 5 Hz	0.13629	ns	N/A
				10 mW, 10 Hz	0.07677	ns	N/A
				10 mW, 15 Hz	0.00124	***	N/A
				10 mW, 20 Hz	0.39782	ns	N/A
				15 mW, 1 Hz	0.00295	***	N/A
				15 mW, 5 Hz	0.03481	*	N/A
				15 mW, 10 Hz	0.00528	**	N/A
				15 mW, 15 Hz	0.39565	ns	N/A
				15 mW, 20 Hz	0.08516	ns	N/A
				20 mW, 1 Hz	0.16659	ns	N/A
				20 mW, 5 Hz	0.00047	†	N/A
				20 mW, 10 Hz	0.39689	ns	N/A
				20 mW, 15 Hz	0.08702	ns	N/A
				20 mW, 20 Hz	0.40124	ns	N/A
fig. S13C	Data in panel B aggregated for individual animal	n=8 mice each group	Mann-Whitney *U* test	Young vs. Aged	0.0002	†	N/A
fig. S13E	Wake duration following optogenetic stimulation during NREM sleep across stimulation parameters: Young vs. Aged	n=8 mice each group	Mann-Whitney *U* test	1 mW, 1 Hz	>0.99999	ns	N/A
				1 mW, 5 Hz	0.01383	*	N/A
				1 mW, 10 Hz	0.00031	†	N/A
				1 mW, 15 Hz	0.00093	****	N/A
				1 mW, 20 Hz	0.34079	ns	N/A
				5 mW, 1 Hz	>0.99999	ns	N/A
				5 mW, 5 Hz	0.01632	*	N/A
				5 mW, 10 Hz	0.00078	****	N/A
				5 mW, 15 Hz	0.09883	ns	N/A
				5 mW, 20 Hz	0.02067	*	N/A

				10 mW, 1 Hz	0.44615	ns	N/A
				10 mW, 5 Hz	0.03465	*	N/A
				10 mW, 10 Hz	0.00699	**	N/A
				10 mW, 15 Hz	0.48967	ns	N/A
				10 mW, 20 Hz	0.00280	***	N/A
				15 mW, 1 Hz	0.08221	ns	N/A
				15 mW, 5 Hz	0.00047	†	N/A
				15 mW, 10 Hz	0.01150	*	N/A
				15 mW, 15 Hz	0.02331	*	N/A
				15 mW, 20 Hz	0.00016	†	N/A
				20 mW, 1 Hz	0.19612	ns	N/A
				20 mW, 5 Hz	0.02409	*	N/A
				20 mW, 10 Hz	0.18617	ns	N/A
				20 mW, 15 Hz	0.02238	*	N/A
				20 mW, 20 Hz	0.02564	*	N/A
fig. S13F	Data in panel E aggregated for individual animal	n=8 mice each group	Mann-Whitney *U* test	Young vs. Aged	0.0002	†	N/A
fig. S13H	Latency for REM-to-wake transition across stimulation parameters: Young vs. Aged	n=8 mice each group	Mann-Whitney *U* test	1 mW, 1 Hz	0.48718	ns	N/A
				1 mW, 5 Hz	0.00295	***	N/A
				1 mW, 10 Hz	0.87848	ns	N/A
				1 mW, 15 Hz	0.04584	*	N/A
				1 mW, 20 Hz	0.01166	*	N/A
				5 mW, 1 Hz	0.32820	ns	N/A
				5 mW, 5 Hz	0.00295	***	N/A
				5 mW, 10 Hz	0.00016	†	N/A
				5 mW, 15 Hz	0.00979	**	N/A
				5 mW, 20 Hz	0.22144	ns	N/A
				10 mW, 1 Hz	0.07786	ns	N/A
				10 mW, 5 Hz	0.00295	***	N/A
				10 mW, 10 Hz	0.00016	†	N/A
				10 mW, 15 Hz	0.26014	ns	N/A
				10 mW, 20 Hz	0.36504	ns	N/A
				15 mW, 1 Hz	0.16908	ns	N/A
				15 mW, 5 Hz	0.00435	***	N/A
				15 mW, 10 Hz	0.00016	†	N/A
				15 mW, 15 Hz	0.81834	ns	N/A
				15 mW, 20 Hz	0.01911	*	N/A
				20 mW, 1 Hz	0.31438	ns	N/A
				20 mW, 5 Hz	0.00016	†	N/A
				20 mW, 10 Hz	0.66356	ns	N/A
				20 mW, 15 Hz	0.19223	ns	N/A
				20 mW, 20 Hz	0.19643	ns	N/A
fig. S13I	Data in panel H aggregated for individual animal	n=8 mice each group	Mann-Whitney *U* test	Young vs. Aged	0.0002	†	N/A
fig. S13K	Wake duration following optogenetic stimulation during REM sleep across stimulation parameters: Young vs. Aged	n=8 mice each group	Mann-Whitney *U* test	1 mW, 1 Hz	>0.99999	ns	N/A
				1 mW, 5 Hz	0.07692	ns	N/A
				1 mW, 10 Hz	0.92820	ns	N/A
				1 mW, 15 Hz	0.57576	ns	N/A
				1 mW, 20 Hz	0.02160	*	N/A
				5 mW, 1 Hz	0.46667	ns	N/A
				5 mW, 5 Hz	0.00140	***	N/A
				5 mW, 10 Hz	0.01181	*	N/A
				5 mW, 15 Hz	0.00155	***	N/A
				5 mW, 20 Hz	0.22378	ns	N/A
				10 mW, 1 Hz	>0.99999	ns	N/A

				10 mW, 5 Hz	0.01321	*	N/A
				10 mW, 10 Hz	0.04087	*	N/A
				10 mW, 15 Hz	0.07817	ns	N/A
				10 mW, 20 Hz	0.00186	***	N/A
				15 mW, 1 Hz	0.07692	ns	N/A
				15 mW, 5 Hz	0.66402	ns	N/A
				15 mW, 10 Hz	0.03512	*	N/A
				15 mW, 15 Hz	0.15229	ns	N/A
				15 mW, 20 Hz	0.77576	ns	N/A
				20 mW, 1 Hz	0.23077	ns	N/A
				20 mW, 5 Hz	0.73908	ns	N/A
				20 mW, 10 Hz	0.77669	ns	N/A
				20 mW, 15 Hz	0.16892	ns	N/A
				20 mW, 20 Hz	0.00295	***	N/A
fig. S13L	Data in panel K aggregated for individual animal	n=8 mice each group	Mann-Whitney *U* test	Young vs. Aged	0.0003	†	N/A

fig. S14

Panel	**Data**	**Group size**	**Statistic method**	**Comparison**	***P* value**	**Notation**	**F/t statistic**
fig. S14D	LC NA resting membrane potential	Young: n=10 vs. Aged: n=13	Mann-Whitney *U* test	Young vs. Aged	0.0666	ns	N/A